

**Rational Design and Preliminary Validation
of Novel Glutaminase C Modulators**

*Submitted in partial fulfilment
of the requirements of the
Degree of Master of Pharmacy*

Lara Zammit

Department of Pharmacy

2021



L-Università
ta' Malta

University of Malta Library – Electronic Thesis & Dissertations (ETD) Repository

The copyright of this thesis/dissertation belongs to the author. The author's rights in respect of this work are as defined by the Copyright Act (Chapter 415) of the Laws of Malta or as modified by any successive legislation.

Users may access this full-text thesis/dissertation and can make use of the information contained in accordance with the Copyright Act provided that the author must be properly acknowledged. Further distribution or reproduction in any format is prohibited without the prior permission of the copyright holder.

Dedicated to my family and closest friends

Abstract

Glutaminolysis is a process which drives cell proliferation in tumours. This process is driven by Glutaminase C (Gc). Literature indicates that Gc is over-expressed in solid tumours mainly those of the lung and that its antagonism could inhibit tumour growth. The objective in this study is to design & identify novel Gc modulators through Virtual Screening (VS) & *de novo* design. The design of this project uses high affinity Gc inhibitor experimental molecule CB-839, used as a lead for the identification of optimised analogues using VS. A consensus pharmacophore was generated by superimposing pharmacophores of inhibitor molecules obtained from PDB crystallographic depositions 5HL1 & 5WJ6 using Ligand Scout[®]. Sybyl-X[®] was used to model a protomol; followed by docking of hits obtained through VS. The ligand binding affinities of the 2 hit molecular structures were calculated in Sybyl-X[®]. The *de novo* approach was used to design novel modulators, where seed structures derived from CB-839 were modelled and allowed growth within the CB-839 ligand binding pocket (LBP). The main outcome of this project is to obtain two molecular cohorts of high affinity lead-like Gc modulators. Through virtual screening, 2 high affinity lead-like molecules were yielded; which are structurally diverse from the lead. CB-839 derived seeds were modelled and will be docked into the Gc LBP in *de novo* phase. This study was valuable in modelling a unique pharmacophore that explored maximal pharmacophoric space using VS. The *de novo* design was used as a complementary approach. The optimal structures will be optimised further.

Acknowledgement Page

As an initial note, I would like to express my sincere gratitude to my supervisor, Dr. Claire Shoemake, for her constant support, guidance and patience in the past five years.

My gratitude is further extended to Professor Lillian Azzopardi, Head of Pharmacy Department and Professor Anthony Serracino Inglott for their continuous encouragement throughout the course.

My gratitude also goes towards the rest of the Pharmacy department for their endless patience and help.

Last but not least, I would like to thank my family and all my closest friends for their endless patience, kindness and support.

Table of Contents

Abstract	iii
Acknowledgement Page	iv
List of Tables & Figures	vii
Chapter 1: Introduction	vii
Chapter 2: Methodology	vii
<i>List of abbreviations</i>	<i>xi</i>
Chapter 1	1
1.1 Lung Cancer	2
1.1.1 <i>Incidence and mortality rate of Lung Cancer</i>	3
1.2 Current Management of Lung Cancer	5
1.2.1 <i>Targeted Therapy</i>	7
1.3 Novel Approach to Lung Cancer	8
1.3.1 <i>KEAP1 Role</i>	8
1.3.2 <i>Glutaminase C Enzymes</i>	8
1.4 Importance of Glutaminase C	9
1.4.1 <i>The Structure of Glutaminase C</i>	9
1.4.2 <i>Endogenous Glutaminase C Agonists</i>	10
1.5 Glutaminase C Antagonists	11
1.6 Glutaminase C Inhibition	12
1.6.1 <i>CB-839 Potential in Management of Lung Cancer</i>	12
1.6.2 <i>CB-839 Bioactive Conformation</i>	14
1.6.3 <i>Limitations of CB-839</i>	15
1.7 Rational Drug Design	15
1.8 Software	16
1.9 Conclusion	18
Chapter 2	19
Methodology	19
2.1 Introduction	20
2.2 PDB Selection	21
2.2.1 Ligand Extraction	23

2.3 Conformational Analysis	24
2.4 Virtual Screening	24
2.4.1 <i>Generation of Pharmacophores</i>	25
2.4.2 <i>Generation of Consensus Pharmacophore</i>	26
2.4.3 <i>Screening for Hit molecules</i>	28
2.4.4 <i>Filtering of Hits</i>	29
2.4.5 <i>Protomol Generation</i>	30
2.5 <i>de novo – Structure Based Drug Design</i>	31
2.5.1 <i>Analysis of 2D and 3D Topology Maps</i>	31
2.5.2 <i>Seed Generation</i>	32
2.5.3 <i>de novo Design</i>	32
2.5.4 <i>Filtration According to Lipinski Rule Compliance</i>	33
Chapter 3	34
Results	34
3.1 <i>Results Obtained from Virtual Screening</i>	35
3.1 <i>Results Obtained from de novo Approach</i>	36
3.2.1 <i>Structure Activity Relationship</i>	36
3.2.2 <i>Seeds Generated from the de novo Method</i>	37
Chapter 4	65
Discussion	65
4.0 <i>Discussion</i>	66
References	74
List of Publications and Abstracts	80

List of Tables & Figures

Chapter 1: Introduction

Table 1.1: Software to be used in the execution of this study	16
Figure 1.1: Incidence and Mortality Rate of Lung Cancer in Men and Women (Wong, Lao & Ho et al., 2017).	5
Figure 1.2: 3-dimensional co-ordinates of Glutaminase-C receptor as described in PDB 5HL1 and rendered in Discovery Studio®	10
Figure 1.3: 2D structure of DON rendered in Accelrys Draw®	11
Figure 1.4: 2D structure of CB-839 rendered in Accelrys Draw®	13
Figure 1.5: 3-dimensional co -ordinates of Glutaminase C receptor bound to the small molecule inhibitor CB-839 as described in PDB crystallographic deposition 5HL1 (Huang & Cerione, 2016) and rendered in Discovery Studio®	14

Chapter 2: Methodology

Table 2.1: Systematic summary regarding the method adopted within this project ..	20
Table 2.2: Lipinski's Rule of 5 Criteria (Lipinski et al., 2015).....	29
Table 2.3: Systematic summary of <i>de novo</i> method.....	31

Table 2.4: Established parameters for novel structure generation using the GROW algorithm.....	33
Figure 2.1: PDB 5HL1 (Huang & Cerione, 2016) describing the Glutaminase C in complex with the inhibitor molecule CB-839 rendered in LigandScout® (Wolber & Langer,2005)	21
Figure 2.2: PDB 5WJ6 (Huang et al., 2018) describing the Glutaminase C with the inhibitor molecule UPGL-0004 rendered in LigandScout® (Wolber & Langer,2005)....	22
Figure 2.3 : Pharmacophore of Glutaminase C docked in 5HL1 (Huang & Cerione, 2016) in rendered in LigandScout® (Wolber & Langer,2005).....	25
Figure 2.4: Pharmacophore of Glutaminase C docked in 5WJ6 (Huang et al., 2018) in rendered in Ligand Scout® (Wolber and Langer, 2005)	26
Figure 2.5: Consensus Pharmacophore of the two pharmacophores extracted from PDB 5HL1 (Huang & Cerione, 2016) and 5WJ6 (Huang et al., 2018) superimposed in Ligand Scout® (Wolber and Langer, 2005).....	27
Figure 2.6: Protomol at the core of Glutaminase C modelled in Sybyl-X® (Certara USA, Inc.)	30

Chapter 3: Results

Table 3.1: Ligands with the highest affinity for the Ligand Binding Pocket obtained through Virtual Screening.....	35
--	----

Table 3.2: Seeds generated from the <i>de novo</i> method rendered in Discovery Studio® and BIOVIA Accelrys Draw®	37
Table 3.3: 2D and 3D structures of the highest affinity generated molecules from seed 1; together with its corresponding properties- rendered in Discovery Studio® and BIOVIA Accelrys Draw®	38
Table 3.4: 2D and 3D structures of the lowest affinity generated molecules from seed 1; together with its corresponding properties- rendered in Discovery Studio® and BIOVIA Accelrys Draw®	48
Table 3.3: 2D and 3D structures of the highest affinity generated molecules from seed 2; together with its corresponding properties- rendered in Discovery Studio® and BIOVIA Accelrys Draw®	54
Table 3.3: 2D and 3D structures of the lowest affinity generated molecules from seed 2; together with its corresponding properties- rendered in Discovery Studio® and BIOVIA Accelrys Draw®	60
Figure 3.1 Topology map generated in PoseView® (Stierand & Rarey, 2010).....	36

Chapter 4: Discussion

Table 4.1: Table comparing <i>de novo</i> and VS approach	66
Table 4.2: Table comparing molecules obtained from Seed 1 with the highest affinity to the ligand binding pocket.....	68
Table 4.3: Table comparing molecules obtained from Seed 2 with the highest affinity to the ligand binding pocket.....	69

Table 4.4: Highest affinity generated molecules from Seed 1 through the <i>de novo</i> approach.....	70
Table 4.5: Highest affinity generated molecules from Seed 2 through the <i>de novo</i> approach.....	70
Figure 4.1: Topology map of PDB crystallographic deposition 5HL1 generated in Discovery Studio®	71
Figure 4.2: Topology map of PDB crystallographic deposition 5WJ6 generated in Discovery Studio®	72
Figure 4.1: Topology map of best <i>de novo</i> molecule C ₂₇ H ₃₈ N ₃ O ₃ generated in Discovery Studio®	72

List of abbreviations

- **ALK** – Anaplastic Lymphoma Kinase
- **ASR** – Age Standardised Rate
- **CoA** – Co-Enzyme A
- **DON** – 6-Diazo-5-oxo-L-norleucine
- **EGRF** – Epidermal Growth Factor Receptor
- **HBA** – Hydrogen acceptor count
- **HBD** – Hydrogen donor count
- **KEAP1** – Kelch-like ECH Associated Protein 1
- **LBE** – Ligand Binding Energy
- **LBP** – Ligand Binding Pocket
- **NFE2L2** – Nuclear Factor Erythroid 2-related 2
- **NMR** – Nuclear Magnetic Radiation
- **PCR** – Polymerase Chain Reaction
- **PDB** – Protein Data Bank
- **VS** – Virtual Screening

Chapter 1

Introduction

1.1 Lung Cancer

Lung cancer is the highest cause of cancer death among men and women. Every year, more men and women die of lung cancer compared to colon, breast and prostate cancer combined. Lung cancer predominantly occurs in the older generation (65 years or older), while a marginal number of patients are diagnosed younger than the age of 45. The average age of lung cancer diagnosis is 70 years.

The overall chance of being diagnosed with lung cancer is 1:15 for men and 1:17 for women. These values include both smokers and non-smokers, however smokers have a greater risk of developing lung cancer. (Wozniak, Gadgeel, 2010).

Cigarette smoking is a significant risk factor for lung cancer. In the US, approximately 80% of lung cancer deaths are caused by smoking. The risk is increased by both quantity and duration (Siegel *et al.*, 2020).

The incidence rate has declined from the 1980's in males and 2000's in females due to gender differences in the smoking uptake and termination patterns. The incidence rate has declined by 4% and 3% per year in males and females respectively (Siegel *et al.*, 2020).

Other factors that increase the risk of lung cancer include exposure to (Wong, Lao & Ho *et al.*, 2017):

- Asbestos
- Chromium & Arsenic

These exposure issues may be avoided therefore, decreasing the risk of developing lung cancer. However, other contributing factors have been identified including genetic, ethnic and racial contributors to the overall risk of lung cancer development. Specifically, epidemiological data indicates that males of African descent are 20% more likely to develop lung cancer than their Caucasian counterparts. Conversely, the incidence of lung cancer is 10% lower in women of African descent compared to their Caucasian counterparts. However, overall, women seem to have a lower risk of developing lung cancer when compared to males, but the gap between the sexes has been observed to be declining. (Wozniak, Gadgeel, 2010).

1.1.1 Incidence and mortality rate of Lung Cancer

Lung cancer is the most predominant form of cancer, having an estimated 1.8 million new cases in 2012, which accounts for 12.9% of new cancer diagnoses.

According to the 'Global Burden of Disease Study 2020', the health-care burden and costs which were credited to lung cancer was highly extensive on a global scale. However, this did not come with the best possible outcome as its 5-year survival rate was only 17.8%. This percentage was much lower than other leading cancers (Wong, Lao & Ho et al., 2017).

In 2012, lung cancer led to 1.6 million deaths. (Ferlay, Shin & Forman, 2010). Therefore, there is a significant scope for research into novel methodologies for the treatment and management of lung cancer.

According to the American Cancer Society, the estimated number of new Lung cancer cases in 2020 is 228,820. Whereas, the number of estimated deaths is 135,720 (Siegel *et al.*, 2020).

Epidemiological studies into the incidence and mortality rates of lung cancer show that the age-standardised rate (ASR) of incidence and mortality was higher in more developed countries. The ASR is expressed per 100,000.

In males, the highest incidence rates of lung cancer were found to be in Central and Eastern Europe having an ASR of 53.5 closely followed by East Asia with an ASR of 50.4. The lowest incidence of lung cancer was found to be in Western Africa with 1.7 (Figure 1.1 – Part A).

On the other hand, in females, the highest incidence of lung cancer was found to be in Northern America where the ASR was estimated to be 33.8 followed by Northern Europe with an ASR value of 23.7. The lowest incidence of lung cancer was found to be in Middle Africa where the ASR was extremely low, standing at a value of 0.8 (Figure 1.1 – Part B).

The mortality rate for males was found to be approximately double than for females. The highest mortality rate for males was found in Central and Eastern Europe (47.6%), whereas in females, the record mortality rates were recorded in North America with 23.5 (Figure 1.1 – Part A & B) (Wong, Lao & Ho *et al.*, 2017).

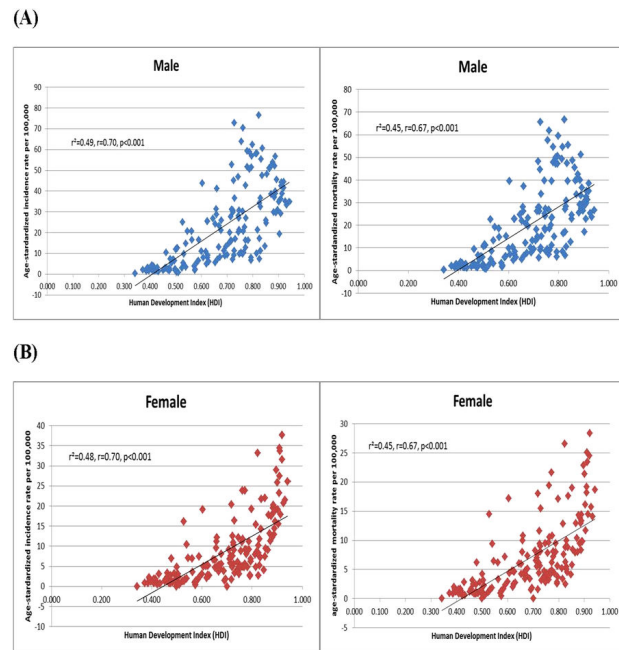


Figure 1.1: Incidence and Mortality Rate of Lung Cancer in Men and Women (Wong, Lao & Ho et al., 2017).

1.2 Current Management of Lung Cancer

The current treatment that is being used to manage lung cancer is:

- Surgery
- Radiofrequency ablation
- Radiation therapy
- Chemotherapy
- Immunotherapy
- Targeted therapy
- Palliative treatment

The treatment used is cancer-type dependent. There are 3 major types of lung cancer:

- i. Lung Carcinoid Tumour
- ii. Small Cell Carcinoma
- iii. Non-Small Cell Carcinoma

The treatment of lung carcinoid tumours entails surgery, chemotherapy, radiation therapy as well as drug treatments such as somatostatin analogs and interferons.

Since Lung Carcinoid Tumours are lung neuro-endocrine tumours; Somatostatin analogs are useful as they slow down the growth of neuro-endocrine cells. Interferons are also useful, as they aid the activation of the immune system which helps to suppress tumour growth. There are also two targeted drugs whose utility in lung cancer management is being evaluated. These are Sunitinib (Sutent[®]) and Everolimus (Afinitor[®]). These drugs are currently being used in the treatment of neuro-endocrine tumours of the pancreas, however are being studied for the use in lung carcinoid tumours.

The treatment of Small Cell Carcinomas entails surgery, chemotherapy and radiation therapy.

The treatment of Non-Small Cell Carcinomas entails surgery, radiofrequency ablation, radiation therapy, chemotherapy, immunotherapy and targeted therapy. (Wozniak, Gadgeel, 2010).

1.2.1 Targeted Therapy

Targeted therapy has been on the rise in the recent years, since researchers have been studying how cells of non-small cell carcinomas grow and divide. Therefore, they have developed new drugs that specifically target changes in cell growth and division.

It is important to note that, targeted therapy works differently from standard chemotherapy. Targeted therapy deals with the certain parts of the cancer cell, hence only destroys the unwanted cells (unlike chemotherapy). Therefore, this means that they will have different side effects, which are usually less severe. Currently, targeted therapy is used for advanced lung cancer, either as mono-therapy or in conjunction with chemotherapy.

There are 4 types of targeted therapy presently being used (Wozniak & Gadgeel, 2010):

- Drugs that target Blood Vessel Growth
- Drugs that target cells with Epidermal Growth Factor Receptor (EGFR) changes
- Drugs that target cells with Anaplastic Lymphoma Kinase (ALK) gene changes
- Drugs that target cells with BRAF gene (encodes protein B-Raf) changes

1.3 Novel Approach to Lung Cancer

1.3.1 KEAP1 Role

Kelch-like ECH associated protein 1 (KEAP1) is a protein that is encoded by KEAP1 gene.

KEAP1 inhibits nuclear factor Erythroid 2-related 2 (NFE2L2- also known as NRF-2) induced cytoprotection. NRF-2 is a 'master regulator of the anti-oxidant response'.

Therefore, it shields against oxidative damage caused by injury and inflammation.

Multiple drugs stimulate NRF-2 pathways for specific diseases that are triggered by stress and toxins (including cancer) (Guo, Yu & Zhang et al., 2015) Henceforth, if KEAP1 inhibits this, there is no cytoprotection, which leads to cancer cell growth. KEAP1 mutations in non-small cell carcinomas have been investigated by reverse transcription Polymerase Chain Reaction (PCR) and Direct Sequencing (Sasaki, Susuki & Shitara et al., 2013)

1.3.2 Glutaminase C Enzymes

Glutaminase is an enzyme, which is responsible for Glutaminolysis. This process involves cancer cells increasing their cell growth and proliferation. Glutaminase is the control of the first step of the Glutaminolysis pathway, which converts Glutamine to Glutamate. Glutamate was identified as the vital part in the use of glutamine by cancer cells.

Therefore, if a drug can inhibit the activity of Glutaminase, the drug would be an outstanding target that would impede cancer cell growth and proliferation.

Three iso-enzymes have been discovered (Thangavelu, Chong & Low *et al.*, 2014):

- i. Kidney-type (KGA/GLS1)
- ii. Liver-type (LGA/GLS2)
- iii. Splice KSA variant (Glutaminase C or GAC)

1.4 Importance of Glutaminase C

Glutaminase C in the evolution of lung cancer is of outmost importance since if this enzyme is inhibited by a drug, this could impede cancer cell growth and spreading in the lung. Henceforth, it is worthwhile to understand this enzyme better. This implies that understanding the structure and function of this enzyme is of significant importance for the identification of small molecules capable of its modulation.

1.4.1 The Structure of Glutaminase C

Evaluation of the X-ray crystal structures of different holo-Glutaminase C complexes (Figure 1.2) indicates that there is a mechanism which involves the 'tetramerization-induced lifting of a gating loop'. This is necessary for its activation through a Phosphate-dependent process. The Phosphate binds inside the catalytic pocket not at the oligomerisation interface. Phosphate also facilitates entry of substrate by competing with glutamate. The greater tendency to oligomerise distinguishes Glutaminase C from the other isoforms. (Cassago, Ferreira & Ferreira, 2012)

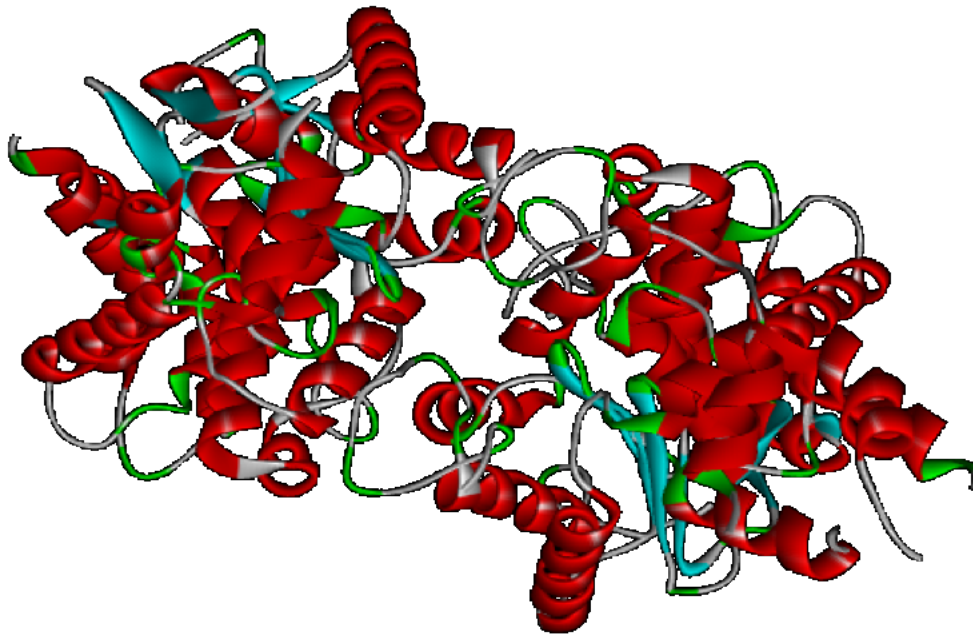


Figure 1.2: 3-dimensional co-ordinates of Glutaminase-C receptor as described in PDB 5HL1 and rendered in Discovery Studio^{® 1}

1.4.2 Endogenous Glutaminase C Agonists

An endogenous agonist is a ligand that is found naturally in the body which binds and activates a receptor. The mechanisms through which Glutaminase C activity is heightened in cancer cells are still not fully understood.

For maximal activity of Glutaminase C-recombinantly expressed, inorganic Phosphate is necessary. This stimulates the conversion of the enzyme dimers into the activated tetramers.

Through several studies, it has been shown that numerous metabolites, such as Acetyl-coA, stimulate Glutaminase activity. However, due to the variation of localisation of

¹Figure of Structure Glutaminase C structure. Available from: <https://www.rcsb.org/structure/5D3O>

Glutaminase C in different tissues, organisms and cell lines, makes it difficult to theorise what endogenously expressed small molecule could act as a Glutaminase C agonist (Katt, Ramachandran & Erickson *et al.*, 2012).

1.5 Glutaminase C Antagonists

6-Diazo-5-oxo-L-norleucine (DON) (Figure 1.3) is an unconventional amino acid, which has a structure similar to that of L-glutamine. This was first isolated in the 1950's from *Streptomyces* bacteria. DON blocks the reactions involving Glutamine in cancer cells (Rais, Jancarik & Tenora *et al.*, 2016). Hence by doing so, terminates cancer cell growth and proliferation. This molecule however had a number of serious adverse effects, which precluded its approval. (Magill, Myers & Reilly *et al.*, 1957) DON was further studied from the point of view of decreasing its systemic side effects. The development of a pro-drug resulted in the development of an entity, which enhanced the therapeutic index and intra-cerebral penetration. (Rais, Jancarik & Tenora *et al.*, 2016)

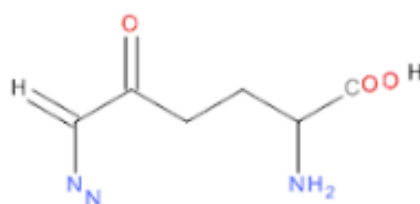


Figure 1.3: 2D structure of DON rendered in Accelrys Draw^{®2}

² Figure of the 2D representation of DON rendered in Accelrys Draw[®] Available from: <http://accelrys.com/products/collaborative-science/biovia-draw/draw-no-fee.php>

1.6 Glutaminase C Inhibition

Given that there is a case to be made for less than perfect Glutaminase C inhibition, the quest for more efficient inhibitors is still present. Recent studies have shown that the small experimental molecule CB-839 shows worthy Glutaminase C inhibition. Furthermore, the CB-839-Glutaminase C complex has been crystallised in the PDB ID 5HL1 (Huang & Cerione, 2016).

1.6.1 CB-839 Potential in Management of Lung Cancer

The systematic name of the molecule CB-839 is N- [5-[4-[6-[[2-[3-(trifluoromethoxy) phenyl] amino]-3-pyridazinyl] butyl]-1,3,4-thiadiazol-2-yl]-2-pyridineacetamide (Figure 1.4).

CB-839 is an inhibitor of Glutaminase C, meaning it inhibits the mitochondrial enzyme Glutaminase C, which is essential for the conversion of Glutamine to Glutamate. This molecule blocks Glutamine usage, therefore impairs the proliferation of cancer cell growth. Glutamine-dependent tumours must undergo the conversion of Glutamine into Glutamate. This is essential to provide energy and for generation building blocks, which are fundamental for the production of macromolecules and tumour proliferation. (Xiang, Stine & Xia, 2015)

Experimental CB-839 (Figure 1.4) is a potent, selective, reversible and orally bioactive molecule. In pre-clinical studies, CB-839 exhibited the inhibition of cancer cell growth and death. This molecule has been established to have anti-tumour activity in various tumour models in animals. It has also been established that animals tolerate CB-839 at concentrations well above those shown to inhibit cancer cell growth.

CB-839 has the potential to impact cancer treatment by;

1. Starving the tumour cell of lung cancer
2. Facilitating the activation of T-cells in the tumour's micro-environment
which is deprived of nutrients

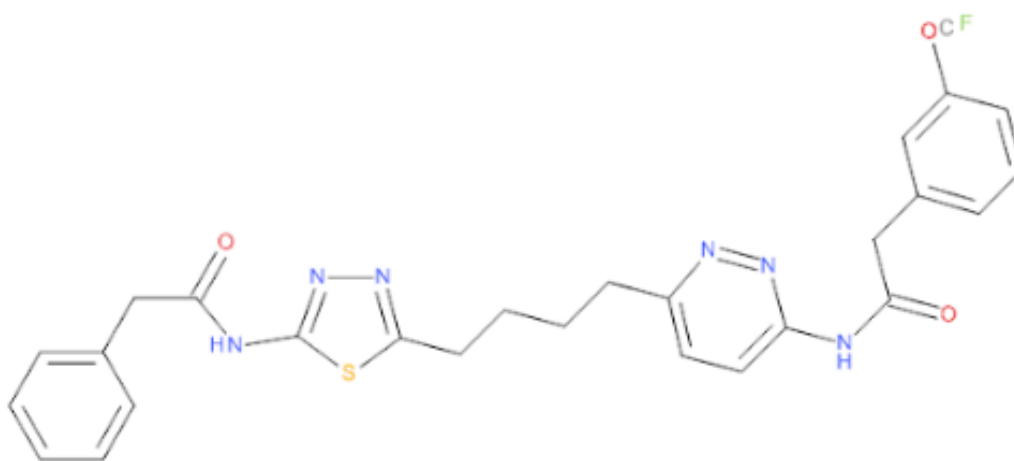


Figure 1.4: 2D structure of CB-839 rendered in Accelrys Draw^{®3}

³ Figure of the 2D representation of CB-839 rendered in Accelrys Draw[®] Available from:
<http://accelrys.com/products/collaborative-science/biovia-draw/draw-no-fee.php>

1.6.2 CB-839 Bioactive Conformation

CB-839 acts as a Hydrolase inhibitor. This molecule has been bound to Glutaminase C as described in the PDB crystallographic deposition 5HL1 (Huang & Cerione, 2016) resolved to an acceptable resolution of 2.4 Ångström (Figure 1.5). It is expressed from *Escherichia Coli* and X-Ray diffraction was used to resolve the protein crystal. (Huang & Cerione, 2016)

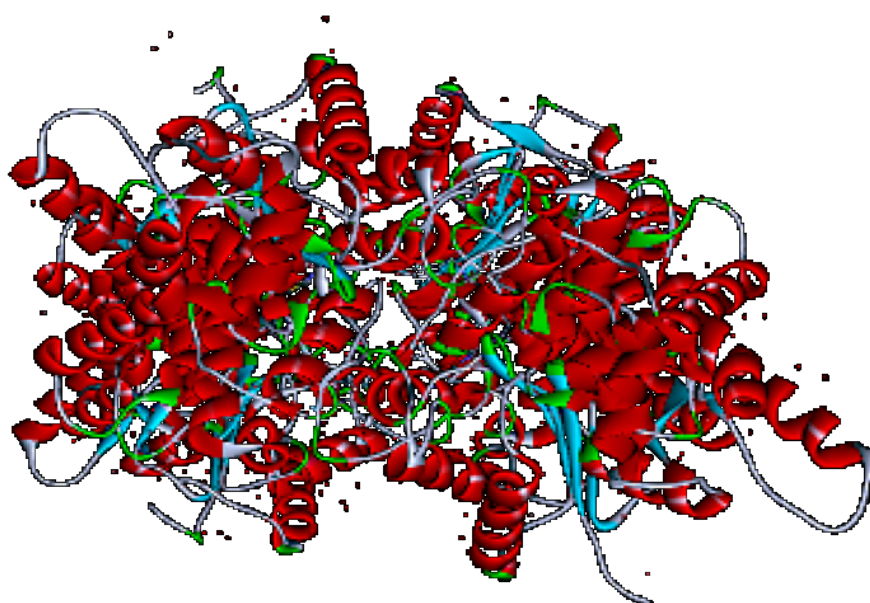


Figure 1.5: 3-dimensional co-ordinates of Glutaminase C receptor bound to the small molecule inhibitor CB-839 as described in PDB crystallographic deposition 5HL1 (Huang & Cerione, 2016) and rendered in Discovery Studio⁴

⁴ Figure of the Structure Glutaminase C receptor bound to small molecule inhibitor CB-839 as described in the PDB crystallographic deposition 5HL1. Available from: <https://www.rcsb.org/structure/5hl1>

1.6.3 Limitations of CB-839

CB-839 is an unstable heat labile molecule which requires to be stored at -20°C. This means constant temperature recording must be done in order to avoid CB-839 not functioning to its optimal potential.

1.7 Rational Drug Design

Drug design aids the understanding of protein structure and physical chemistry. Algorithms of protein design have been beneficial to devise proteins that fold, catalyse and take up their most fitting conformational state (Tiwari *et al.*, 2012).

First, a bio-molecular target of potential therapeutic value needs to be identified. Subsequently, a multidisciplinary team must be formed with the objective of looking for clinical candidates/drug-like compounds that are set for human clinical trials. These compounds are typically selectively bound to the molecular target and tamper either with its activity as a receptor or enzyme. Screening of molecular libraries and optimization of leads is done (Jorgensen, 2004).

The structure of the crystals is determined by methods such as:

- X-ray crystallography
- Nuclear magnetic radiation (NMR)
 - This is less used nowadays

1.8 Software

The software used in this study include (Table 1.1):

Table 1.1: Software to be used in the execution of this study

1. Sybyl-X [®]
2. Discovery Studio [®]
3. LigandScout [®]
4. ZINCpharmer [®]
5. Molsoft [®]
6. Chimera [®]
7. VMD [®]
8. Poseview [®]
9. LigBuilder [®]

Sybyl-X[®] is used to model molecules, which includes both small and macromolecules. The software then simulates them in different environments. From this, one can predict safety issues, identify leads and execute lead optimization using a multitude of QSAR methods.

Discovery Studio[®] is developed and distributed by Accelrys[®]. This is a software company, which accommodates many pharmaceutical and chemical industries. Discovery Studio[®] is able to cover simulation, ligand design, pharmacophore modelling, structure-based design, macromolecule design and validation, macromolecule engineering, QSAR, ADME, and predictive toxicity.

LigandScout[®] is a software which produces 3D pharmacophore models from structural data of macromolecule-ligand complexes. It has been used to forecast new structures in drug design. (Wolber G, Kosara R., 2004)

ZINCpharmer[®] is a free pharmacophore search software. It can import pharmacophore definitions from LigandScout[®] and MOE (Molecular Operating Environment). (Koes & Camacho, 2012)

Molsoft[®] products can aid mainly viewing and docking of molecules, virtual screening, QSAR and lead optimization, molecular modelling and simulations, and structure prediction and mutational analysis.

Chimera[®] is a program which deals with the analysis of molecular conformations and interactive visualisations. These include docking results and density maps.

Poseview[®] is a tool which exhibits molecular complexes which incorporates simplistic ligand and amino acid arrangements towards which it forms interactions (Stierand & Rarey, 2010)

LigBuilder[®] is a software in which allows the analysis of designed compounds; which is able to detect positions and shapes of the surface's binding site of a given protein structure. Also, qualitatively estimates the molecules' drugability. (Vuan, Pei & Lai, 2011)

1.9 Conclusion

A review of the literature emphasises the fact that adenocarcinoma of the lung is still associated with a high mortality rate. Furthermore, it has a relatively high incidence of 1 in every 15 males and 1 in every 17 females, which implies the need for further research into its management.

Literature also indicates that there are novel targets that may be investigated for the development of novel pharmacotherapeutic agents capable of slowing down lung cancer progression. In this review, Glutaminase C expressed as a result of KEAP1 mutation is an example of this. This receptor has already been crystallised and described with its 3-dimensional co-ordinates bound to the small molecule of interest CB-839 being described in the PDB crystallographic deposition 5HL1 (Huang & Cerione, 2016). This means that there is an in-depth understanding of the bioactive conformation of a novel Glutaminase C inhibitor and of the critical interactions that it forges with the amino acid side chains, which line the Glutaminase C ligand binding pocket. This available data creates a robust starting point for this study, which consequently aims to analyse the critical interactions forged between CB-839 and the Glutaminase receptor. It also aims to use these in Virtual Screening and *de novo* approaches to identify and design CB-839 novel analogs with:

- Acceptable oral bioavailability
- Superior interaction with the Glutaminase C receptor

The optimal structures obtained through each approach will further be validated and re-modelled prior to selection for molecular dynamics simulation studies.

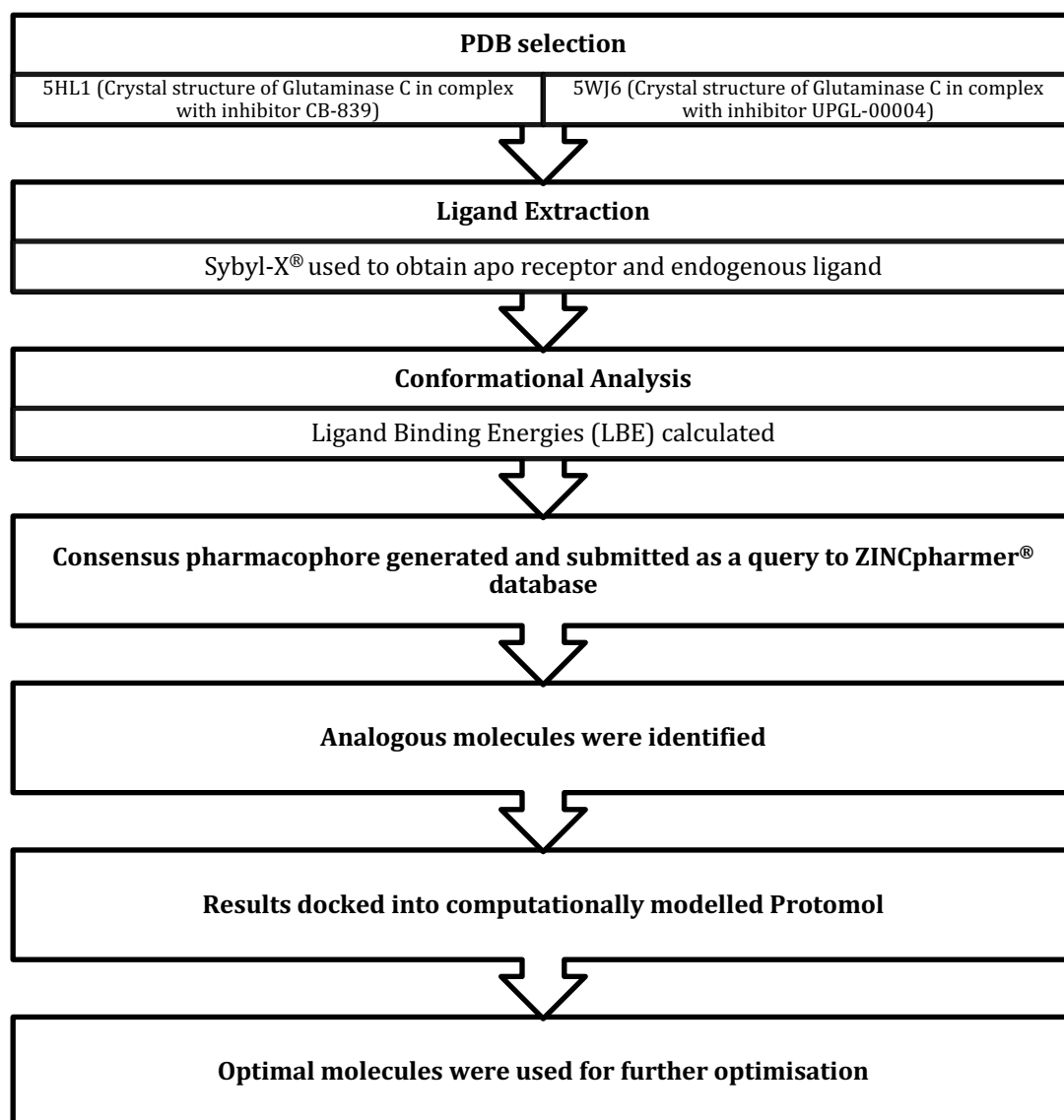
Chapter 2

Methodology

2.1 Introduction

Experimental molecule, CB-839, is a high affinity Glutaminase C inhibitor and was used as a lead molecule in this *in silico* study for the design and identification of optimised analogs (Vogl *et al.*, 2019). The following (Table 2.1) is a systematic summary of the method adopted within this project:

Table 2.1: Systematic summary regarding the method adopted within this project



2.2 PDB Selection

Two PDB crystallographic depositions were considered pertinent to the carrying out of the study. These were 5HL1 (Huang & Cerione, 2016) and 5WJ6 (Huang *et al.*, 2018).

Protein Data Bank (PDB) crystallographic deposition 5HL1 (Huang & Cerione, 2016) describes the crystal structure of Glutaminase C in complex with the inhibitor molecule CB-839. This molecule was resolved through X-ray diffraction to 2.4Å.

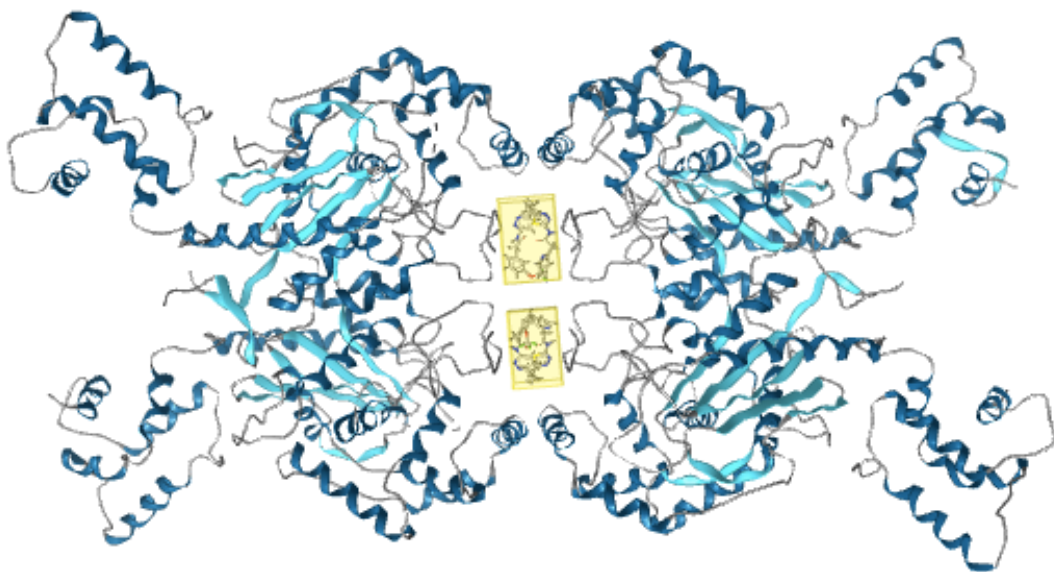


Figure 2.1: PDB 5HL1 (Huang & Cerione, 2016) describing the Glutaminase C in complex with the inhibitor molecule CB-839 rendered in LigandScout® (Wolber & Langer, 2005)

PDB crystallographic deposition 5WJ6 (Huang *et al.*, 2018) describes the crystal structure of Glutaminase C with inhibitor 2-phenyl-N-{5-[4-({5-[(phenylacetyl)amino]-1,3,4-thiadiazol-2-yl}amino)piperidin-1-yl]-1,3,4-thiadiazol-2-yl}acetamide (UPGL-00004). This molecule was resolved through X-ray diffraction to 2.44Å.

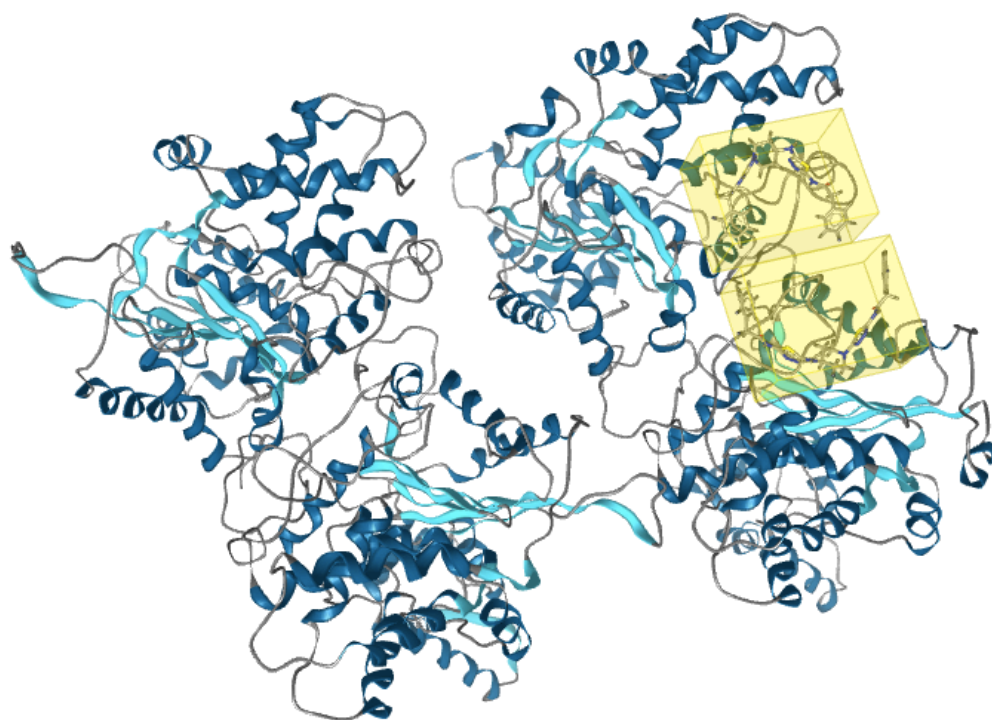


Figure 2.2: PDB 5WJ6 (Huang *et al.*, 2018) describing the Glutaminase C with the inhibitor molecule

UPGL-0004 rendered in LigandScout® (Wolber & Langer, 2005)

2.2.1 Ligand Extraction

Sybyl-X[®] (Certara USA, Inc.) was used for molecular visualisation and modelling. Molecular modelling was used in order to obtain the *apo* receptor and the endogenous ligand.

As an initial step, the bound small molecules were removed from each receptor. This process yielded the bioactive conformation of the bound small molecules at the *apo* cognate receptor in each case. Molecular simplification was then carried out. This process involved the removal of any molecules which were not considered critical to ligand binding and included water molecules lying at a distance greater than 5Å from the ligand binding pocket or any co-crystallised molecules which were described in the literature as not facilitating ligand binding. This process was carried out to enhance visualisation and computational speed.

The extracted small molecules were exported as *mol2* files, whereas their respective *apo* receptors were saved in PDB format.

2.3 Conformational Analysis

Sybyl-X[®] (Certara USA, Inc.) was used in order to generate conformers. This was done by using the 'Similarity Suite' algorithm. Different conformers resulted due to the various rotations of single bonds and rings. The lead molecule was allowed motion and the top 20 binding conformers were selected. The Ligand Binding Energies (LBE) (Kcalmol⁻¹) were calculated using Sybyl-X[®] (Certara USA, Inc.).

This was computed by the addition of the sums of the following different energy values;

- i. Out of Plane Bending Energy
- ii. Van der Waals Energy
- iii. Angle Bending Energy
- iv. Torsional Energy
- v. Bond stretching energy

2.4 Virtual Screening

Virtual Screening is a computational technique used to obtain new molecules with similar three-dimensional spatial orientation and outer electronic structure to the ligand used as a template.

The use of Virtual Screening is based on the fact that molecules having similar structures should exhibit similar effects on the same target molecule (Passeri, 2018).

In this study, the ligand CB-839 was used as a template.

2.4.1 Generation of Pharmacophores

A pharmacophore is explained as an 'ensemble of steric and electronic features that are necessary to ensure the optimal supra-molecular interactions with a specific biologic target and to trigger its biologic response' (Proekt & Hemmings, 2013).

LigandScout® (Wolber and Langer, 2005) was used to generate pharmacophores.

Structure-based approach was used to analyse the essential characteristics such as Hydrogen bonding. This eventually produced three-dimensional pharmacophores.

PDB crystallographic deposition 5HL1 (Huang & Cerione, 2016) was read into Ligand Scout® (Wolber & Langer, 2005), where a 'Macromolecular View' was obtained as well as the coordinates of its bound ligands were generated.

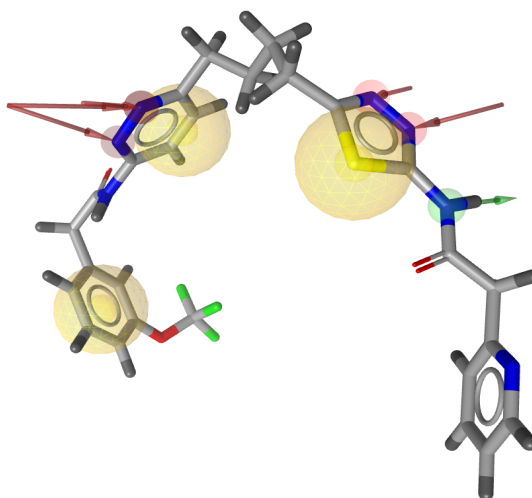


Figure 2.3 : Pharmacophore of Glutaminase C docked in 5HL1 (Huang & Cerione, 2016) in rendered in LigandScout® (Wolber & Langer,2005)

PDB crystallographic deposition 5WJ6 (Huang *et al.*, 2018) was then read into Ligand Scout® (Wolber & Langer, 2005), where the same steps were repeated.

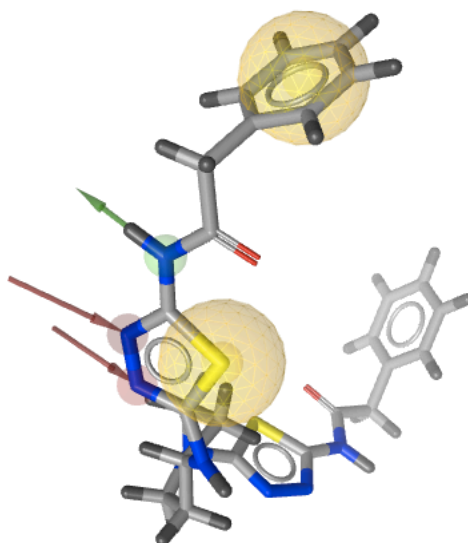


Figure 2.4: Pharmacophore of Glutaminase C docked in 5WJ6 (Huang *et al.*, 2018) is rendered in Ligand Scout® (Wolber and Langer, 2005)

2.4.2 Generation of Consensus Pharmacophore

Pharmacophores for the inhibitors extracted from PDB crystallographic depositions 5HL1 (Huang & Cerione, 2016) and 5WJ6 (Huang *et al.*, 2018) were generated in the previous step.

Pharmacophores of these ligands were superimposed and an average consensus pharmacophore was created incorporating the critical contact points forged by all the component molecules. The consensus pharmacophore (Figure 2.5) was then chosen as the query structure for the upcoming phase of the study.

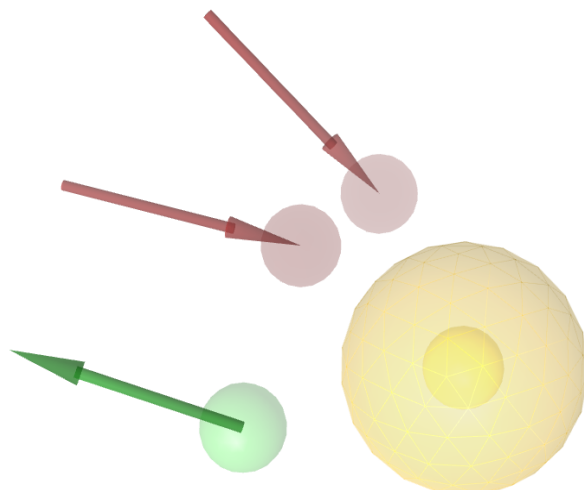


Figure 2.5: Consensus Pharmacophore of the two pharmacophores extracted from PDB 5HL1 (Huang & Cerione, 2016) and 5WJ6 (Huang et al., 2018) superimposed in Ligand Scout® (Wolber and Langer, 2005)

Each colour in Figure 2.5 represents a different interaction:

- **Yellow** – Hydrophobic Interactions
- **Red** – Hydrogen Bond Acceptors
- **Green** – Hydrogen Bond Donors

2.4.3 Screening for Hit molecules

The consensus pharmacophore, which was generated in the previous step as a query structure, was loaded onto the ZINCpharmer[®] (Koes & Camacho, 2012) online database.

The virtual screening process used various filters to ensure lead-like molecules were obtained. The filters below were applied to all, where the hits were then saved in *.sdf* format:

- Maximum total number of hits: 300
- Maximum Root Mean Squared Deviation: 1
- Molecular weight: $1 \leq X \leq 300$
- Rotatable bonds: $1 \leq X \leq 5$

The hits were yielded using 3 databases (last updated in 2014):

- i. ZINC Purchasable Database
- ii. ZINC Natural Products Database
- iii. ZINC Drug Database

A total of 372 hit molecular structures were generated in ZINCpharmer[®] (Koes & Camacho, 2012) which were then imported into MONA[®] (Hilbig & Rarey, 2015).

2.4.4 Filtering of Hits

MONA[®] (Hilbig & Rarey, 2015) was used for further filtration of hits. Filtration was done in order to identify molecules with:

- Drug-like Pharmacological Activities
- Drug-like Physiochemical Activities
- Drug-like Biological Activities

This was carried out according to Lipinski's Rule of 5 (Lipinski *et al.*, 2015), thus the following criteria (Table 2.2) was abided by;

Table 2.2: Lipinski's Rule of 5 Criteria (Lipinski et al., 2015)

Hydrogen Acceptors	1 – 10
Hydrogen Donors	1 – 5
Log P	-1 – 5
Molecular Weight	0 – 500

2.4.5 Protomol Generation

Sybyl-X[®] (Certara USA, Inc.) was used in order to model the protomol. A protomol (or idealised binding site) represents the energetically unsatisfied amino acids at the core of the Glutaminase C receptor.

The protomol generated was used as a docking perimeter for the hits which were identified in the software MONA[®] (Hilbig & Rarey, 2015). The 'Surflex Simulation' function was used in Sybyl-X[®] (Certara USA, Inc.) to create the protomol.

These hits were classified according to their affinity and the optimal structure will be identified.

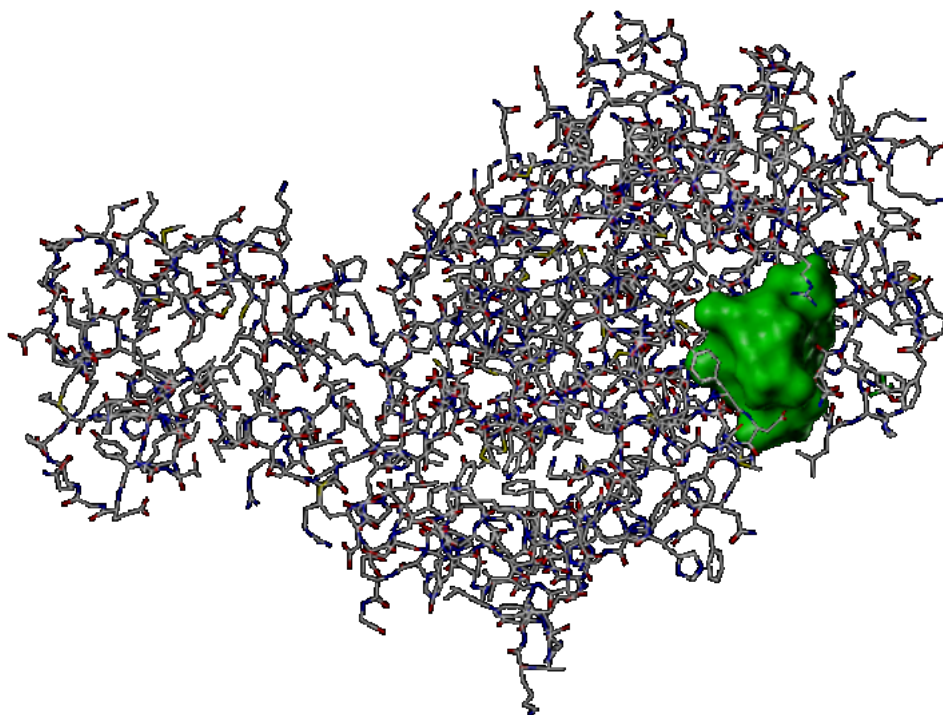
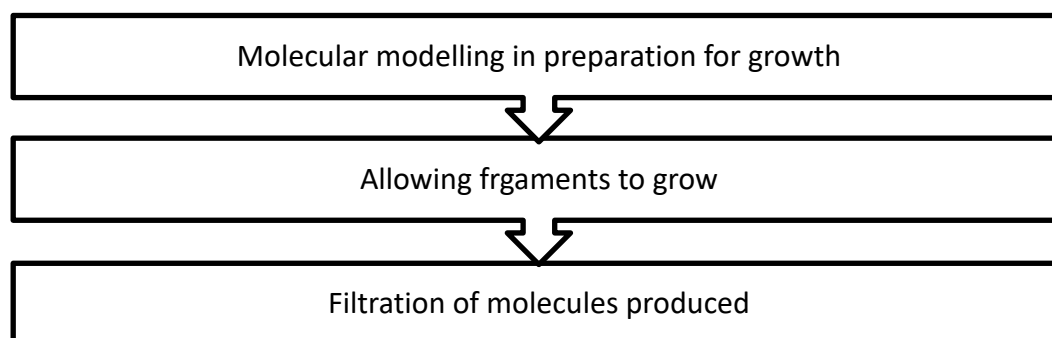


Figure 2.6: Protomol at the core of Glutaminase C modelled in Sybyl-X[®] (Certara USA, Inc.)

2.5 *de novo* – Structure Based Drug Design

Table 2.3: Systematic summary of the *de novo* method



The fundamental step in this method was to identify all the moieties existing on the ligands which are responsible for forging the interaction with the ligand binding pocket, hence creating a biological response.

2.5.1 Analysis of 2D and 3D Topology Maps

The interactions between CB-839 and Glutaminase C were visualised by means of the web-based application, PoseView® (Stierand & Rarey, 2010).

PDB crystallographic deposition 5HL1 (Huang & Cerione, 2016), representing the Glutaminase C receptor in complex with CB-839 was uploaded. An image was generated depicting the various interactions essential for biological activity. Through this process, the critical moieties were identified.

2.5.2 Seed Generation

The fragmentation exercise was carried out on the structure of the ligand, by the removal of any atoms that were shown to be irrelevant to ligand stabilisation through visualisation of the complex in PoseView® (Stierand & Rarey, 2010). The growing sites were assigned on the generated fragments through the designation of H.*spc* atoms in Sybyl-X® (Certara USA, Inc.).

2.5.3 *de novo* Design

De novo drug design is a procedure which uses the receptor's 3D structure to model novel lead molecules by growing and synthesis molecules computationally.

de novo growth was sustained using new lead molecules were created using the GROW function of LigBuilder® (Wang *et al.*, 2000). This function allowed for the detection of the H.*spc* atoms and the addition of various moieties to them according to a methodology that considered spatial orientation and synthetic feasibility. The *de novo* growth process was followed by the organisation, for each seed structure, of the *de novo* generated molecules into families based on pharmacophoric similarity and ligand binding affinity. This latter procedure was carried out using the process module of LigBuilder® (Wang *et al.*, 2000).

The GROW algorithm was run for each structure accordingly. However, molecular growth was restricted by parameters shown in Table 2.4, which are pre-set by LigBuilder® (Wang *et al.*, 2000).

*Table 2.4: Established parameters for novel structure generation
using the GROW algorithm*

Parameter	Value
Maximum Molecular Weight	600
Minimum Molecular Weight	300
Maximum LogP	6
Minimum LogP	3
Maximum Hydrogen Bond Donor	6
Minimum Hydrogen Bond Donor	2
Maximum Hydrogen Bond Acceptor	6
Minimum Hydrogen Bond Acceptor	2
Maximum pKd	10
Minimum pKd	5

2.5.4 Filtration According to Lipinski Rule Compliance

The filtering process of the de novo structures were filtered two-fold.

Firstly, the molecules were filtered according to molecular weight and pKd, where in this first process, 38.5% and 47% for Seed 1 and 2 respectively were discarded.

The second part of the filtration process was by determining the Hydrogen Acceptor count (HBA) and Hydrogen Donor count (HBD). This process yielded a small number of molecules discarded.

Chapter 3

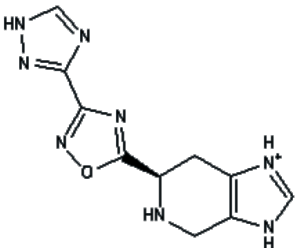
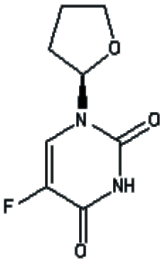
Results

3.1 Results Obtained from Virtual Screening

The Lipinski Rule compliant ligands which were obtained from ZINCpharmer® (Koes & Camacho, 2015) were docked into the protomol seen in Figure 2.6. These were then ranked according to affinity for the protomol, as seen in Table 3.1.

Table 3.1: Ligands with the highest affinity for the Ligand Binding Pocket

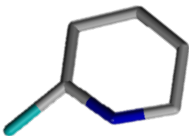
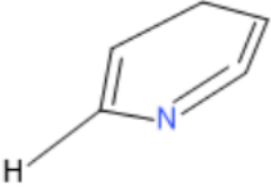
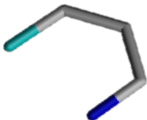
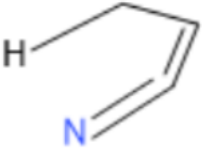
obtained through Virtual Screening

ZINCpharmer® ligand ID	Total score
 ZINC9277850	7.17
 ZINC00119895	1.53

3.2.2 Seeds Generated from the *de novo* Method

Table 3.2: Seeds generated from the *de novo* method rendered in Discovery Studio⁵ and BIOVIA

Accelrys Draw⁶

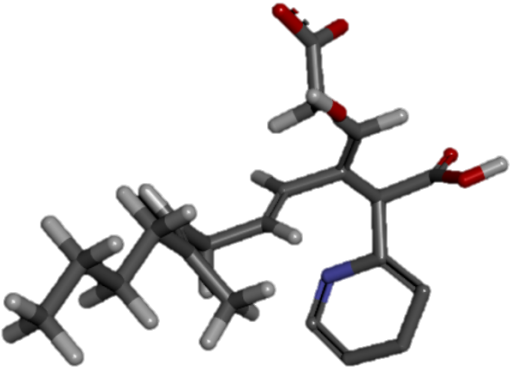
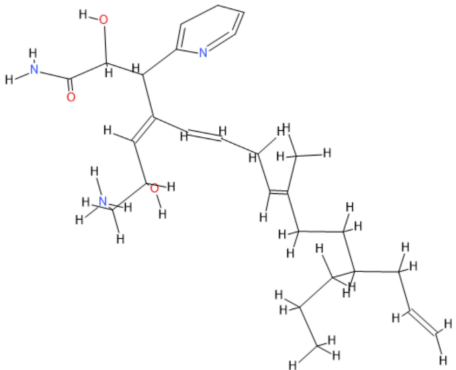
Seed	3D Structure	2D Structure
Seed 1		
Seed 2		

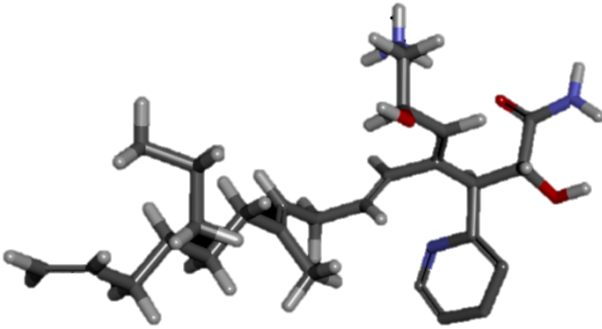
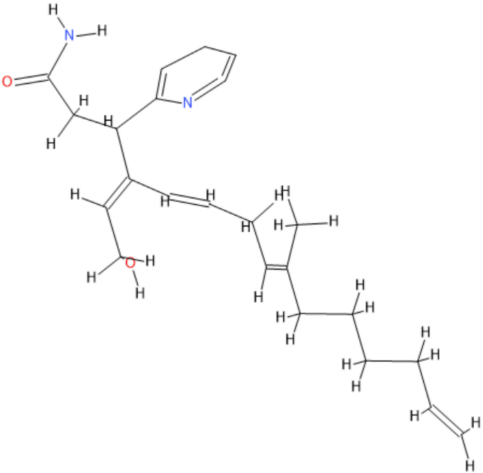
The seeds in table 3.2 were successfully grown within the ligand binding pocket. Each seed generated two-hundred ligands. These were further filtered according to Lipinski's Rule.

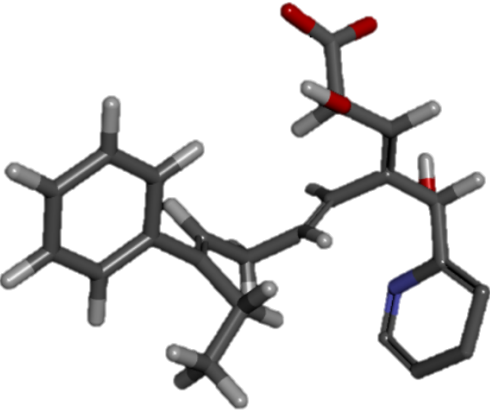
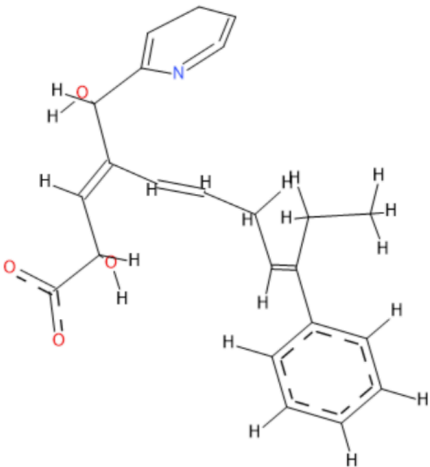
⁵ Dassault Systèmes. BIOVIA Discovery Studio Visualizer. Version 20.1 [software]. Dassault Systèmes. 2020 [cited 2021 Jul 14; downloaded 2021 March 2]. Available from: <https://www.3dsbiovia.com/products/collaborative-science/biovia-discovery-studio/visualization-download.php>.

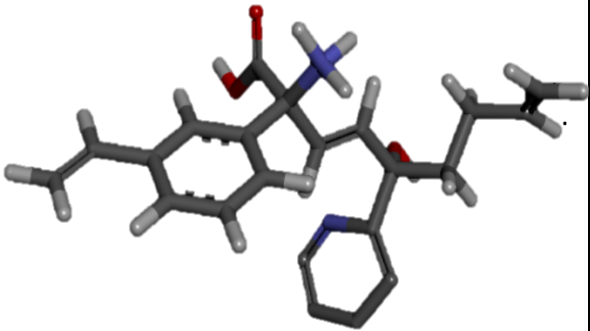
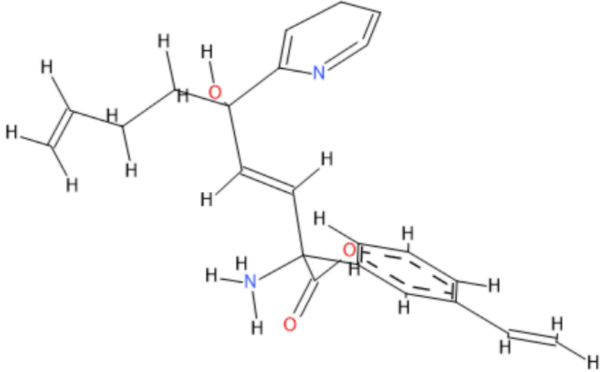
⁶ Accelrys Draw[®] Available from: <http://accelrys.com/products/collaborative-science/biovia-draw/draw-no-fee.php>

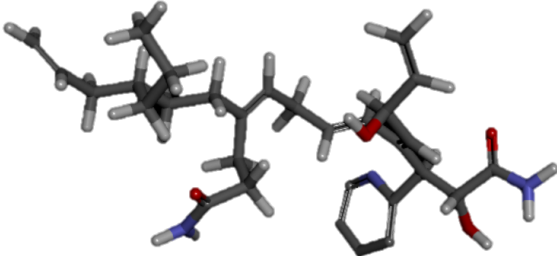
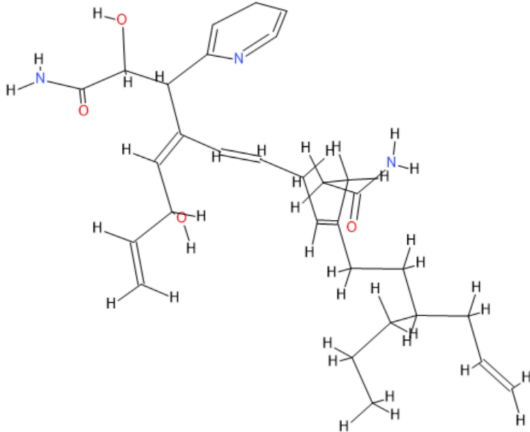
Table 3.3: 2D and 3D structures of the **highest** affinity generated molecules from **Seed 1**; together with its corresponding properties - rendered in Discovery Studio^{®5} and BIOVIA Accelrys Draw^{®6}

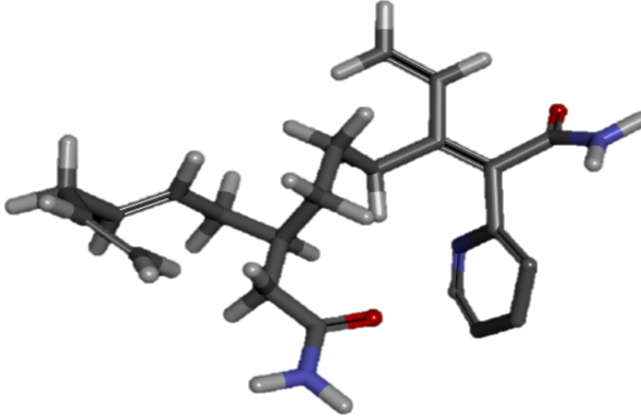
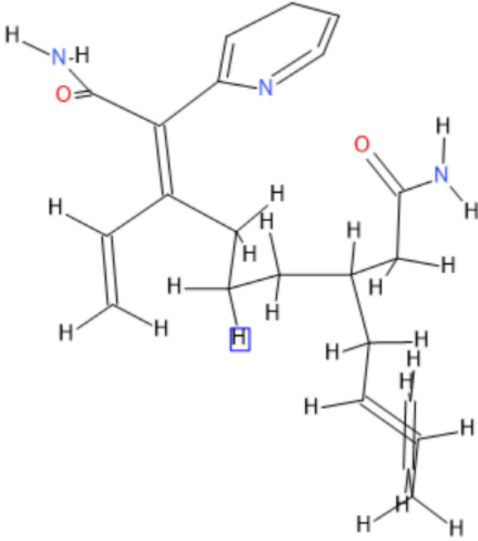
Structure	Family 1	Properties
3D		<p>Molecular weight: 452</p> <p>LogP: 4.48</p> <p>pKd: 9.98</p> <p>HBA: 4</p> <p>HBD: 4</p>
2D		

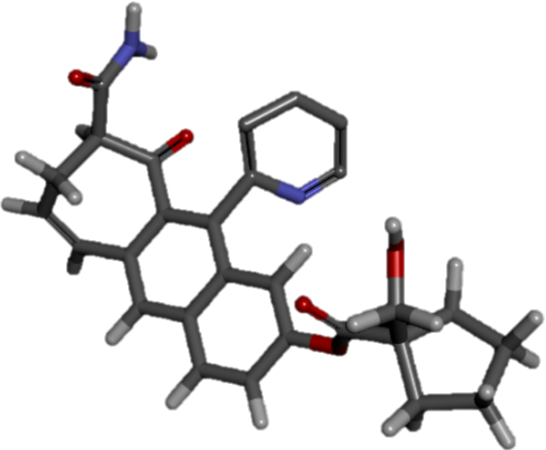
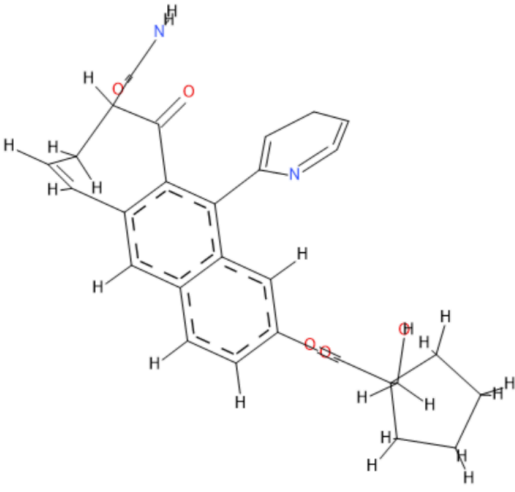
Structure	Family 2	Properties
3D		<p data-bbox="1091 808 1390 842">Molecular weight: 365</p> <p data-bbox="1091 889 1209 922">LogP: 4.7</p> <p data-bbox="1091 969 1214 1003">pKd: 9.18</p> <p data-bbox="1091 1050 1177 1084">HBA: 3</p> <p data-bbox="1091 1131 1177 1164">HBD: 2</p>
2D		

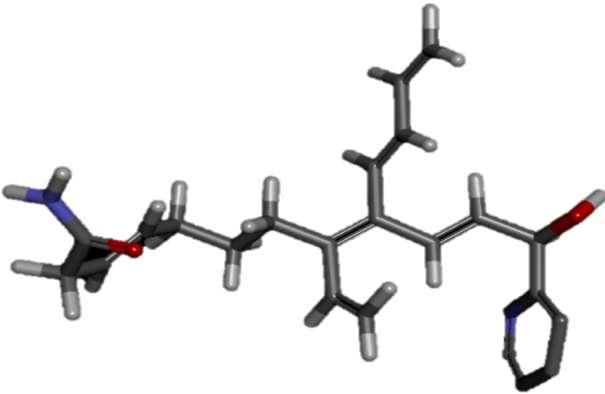
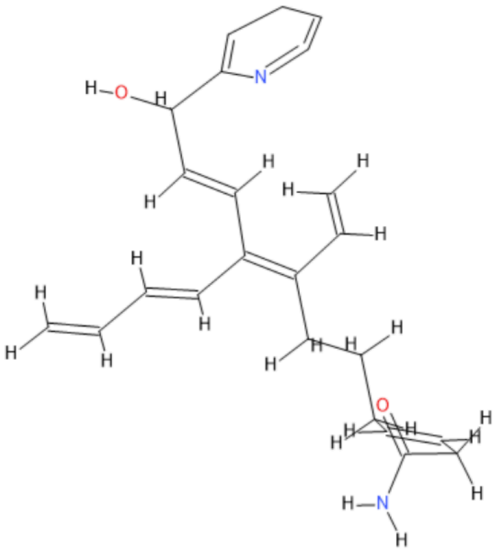
Structure	Family 4	Properties
3D		<p>Molecular weight: 374</p> <p>LogP: 4.56</p> <p>pKd: 8.58</p> <p>HBA: 5</p> <p>HBD: 3</p>
2D		

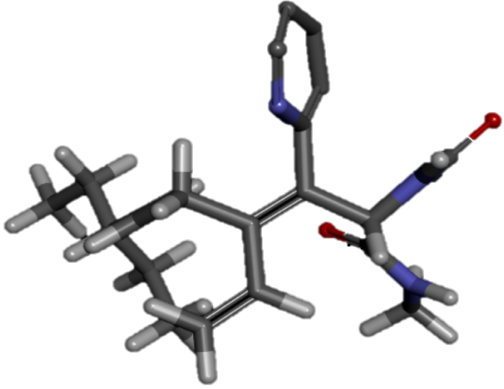
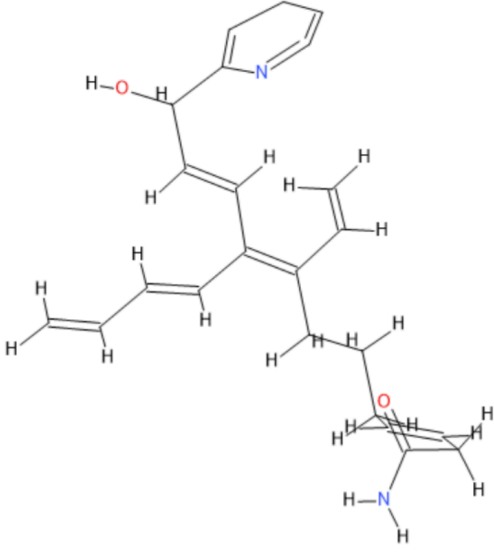
Structure	Family 5	Properties
3D		<p>Molecular weight: 361</p> <p>LogP: 3.07</p> <p>pKd: 9.63</p> <p>HBA: 4</p> <p>HBD: 3</p>
2D		

Structure	Family 6	Properties
3D		<p>Molecular weight: 433</p> <p>LogP: 4.28</p> <p>pKd: 9.63</p> <p>HBA: 5</p> <p>HBD: 4</p>
2D		

Structure	Family 7	Properties
3D		<p data-bbox="1102 808 1401 842">Molecular weight: 363</p> <p data-bbox="1102 887 1241 920">LogP: 4.46</p> <p data-bbox="1102 965 1230 999">pKd: 8.58</p> <p data-bbox="1102 1043 1193 1077">HBA: 3</p> <p data-bbox="1102 1122 1193 1155">HBD: 2</p>
2D		

Structure	Family 9	Properties
3D		<p>Molecular weight: 466</p> <p>LogP: 4.94</p> <p>pKd: 9.28</p> <p>HBA: 6</p> <p>HBD: 2</p>
2D		

Structure	Family 11	Properties
3D		<p>Molecular weight: 360</p> <p>LogP: 4.63</p> <p>pKd: 8.74</p> <p>HBA: 3</p> <p>HBD: 2</p>
2D		

Structure	Family 12	Properties
3D		<p>Molecular weight: 351</p> <p>LogP: 4.67</p> <p>pKd: 8.47</p> <p>HBA: 3</p> <p>HBD: 2</p>
2D		

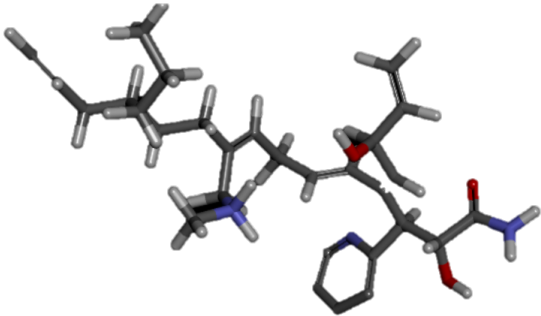
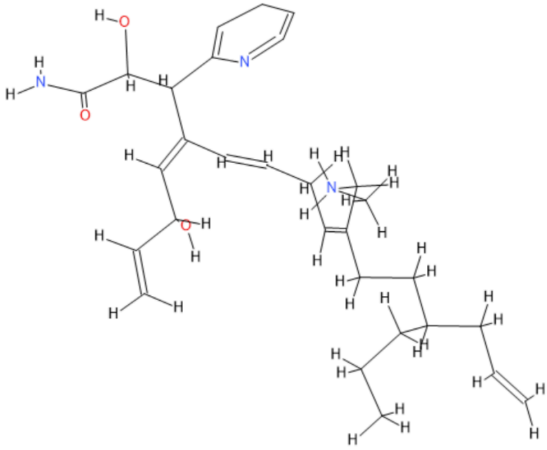
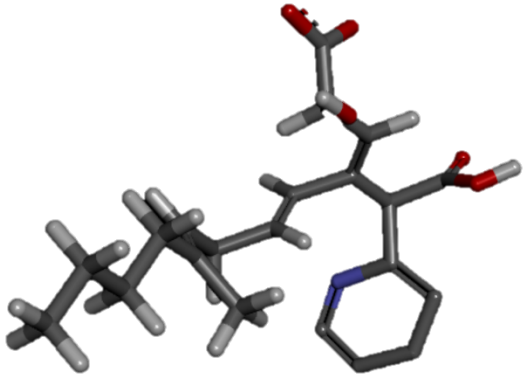
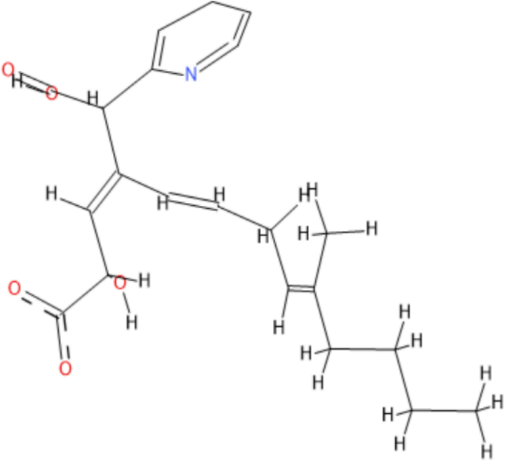

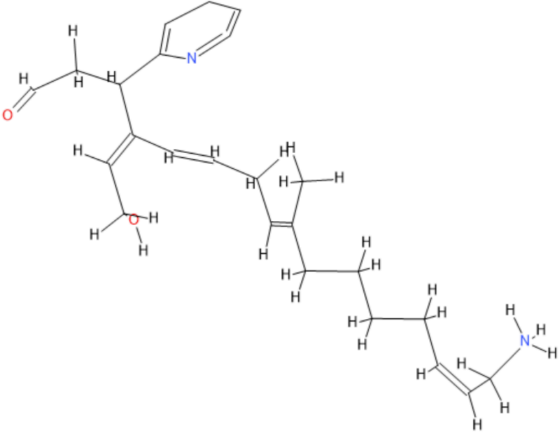
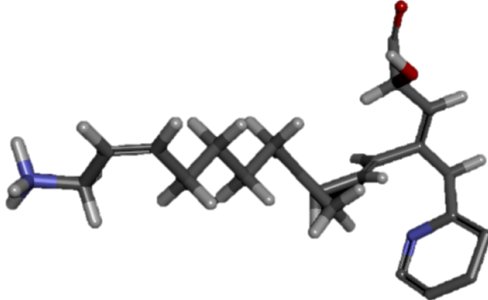
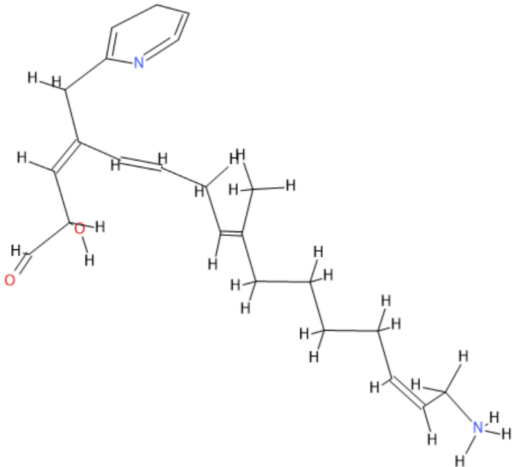
Structure	Family 13	Properties
3D		<p>Molecular weight: 309</p> <p>LogP: 4.5</p> <p>pKd: 9</p> <p>HBA: 4</p> <p>HBD: 4</p>
2D		

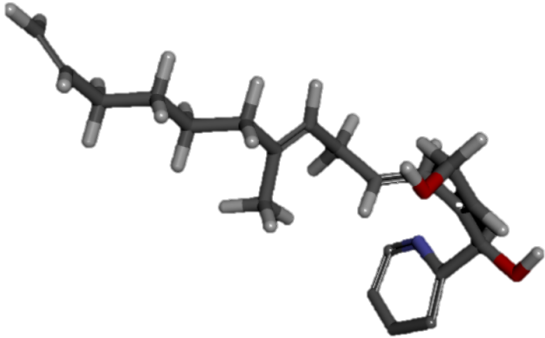
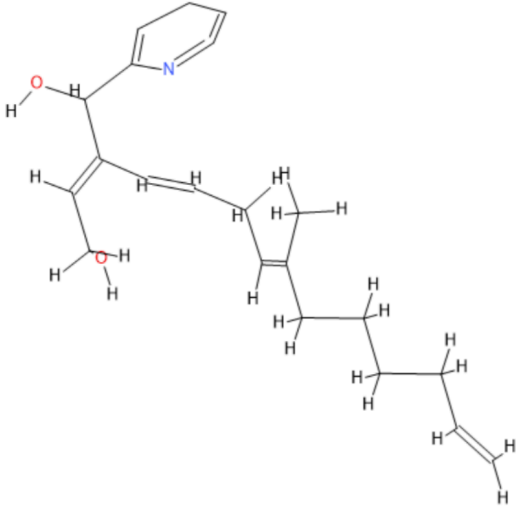
Table 3.4: 2D and 3D structures of the **lowest** affinity generated molecules from **Seed 1**; together with its corresponding properties. Images rendered in Discovery Studio^{®5} and BIOVIA Accelrys

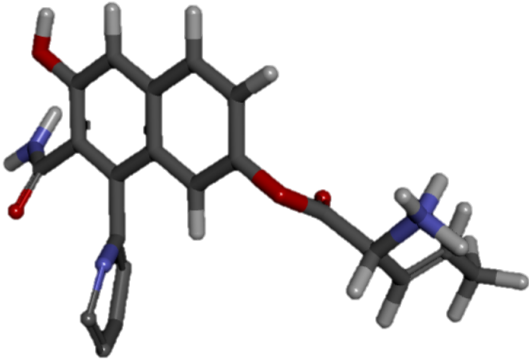
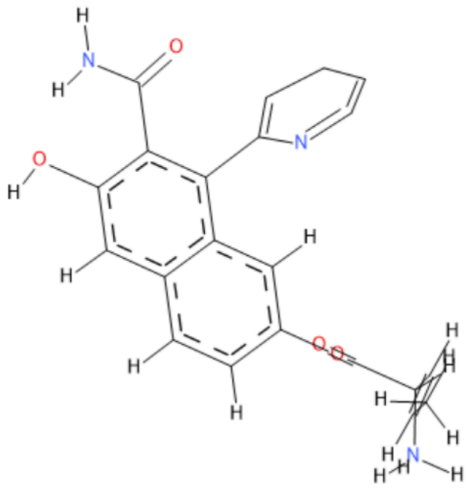
Draw^{®6}

Structure	Family 1	Properties
3D		<p>Molecular weight: 368</p> <p>LogP: 3.72</p> <p>pKd: 8.43</p> <p>HBA: 6</p> <p>HBD: 3</p>
2D		

Structure	Family 2	Properties
3D		<p>Molecular weight: 368</p> <p>LogP: 3.72</p> <p>pKd: 8.43</p> <p>HBA: 6</p> <p>HBD: 3</p>
2D		

Structure	Family 4	Properties
3D		<p>Molecular weight: 388</p> <p>LogP: 4.75</p> <p>pKd: 8.41</p> <p>HBA: 3</p> <p>HBD: 2</p>
2D		

Structure	Family 6	Properties
3D		<p>Molecular weight: 335</p> <p>LogP: 4.89</p> <p>pKd: 8.41</p> <p>HBA: 3</p> <p>HBD: 2</p>
2D		

Structure	Family 9	Properties
3D		<p>Molecular weight: 374</p> <p>LogP: 4.36</p> <p>pKd: 8.65</p> <p>HBA: 5</p> <p>HBD: 3</p>
2D		

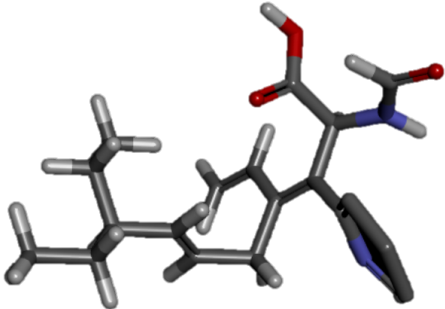
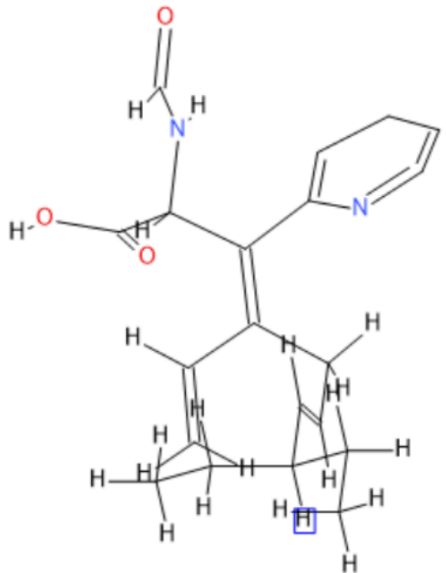
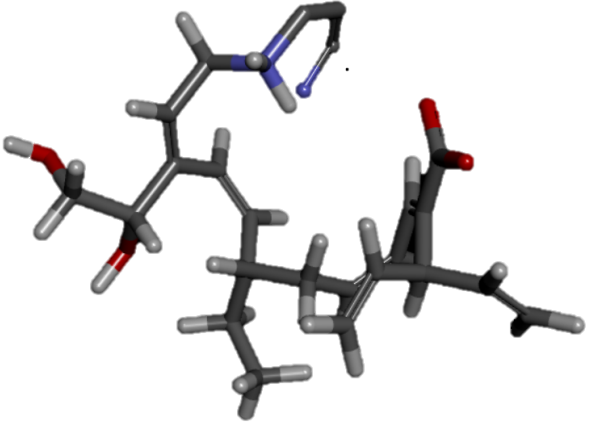
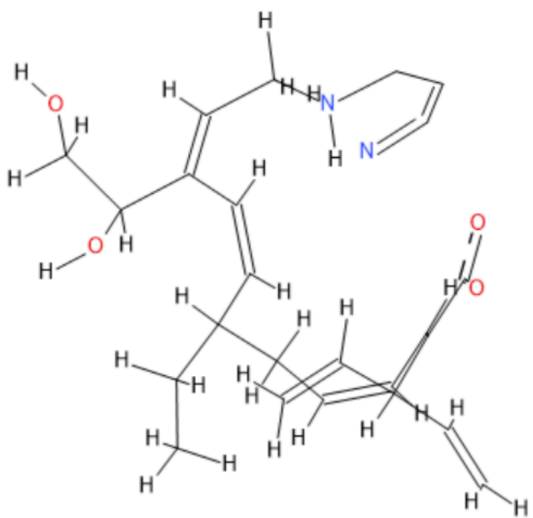
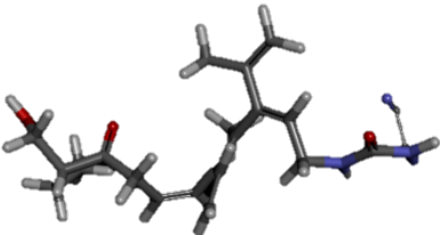
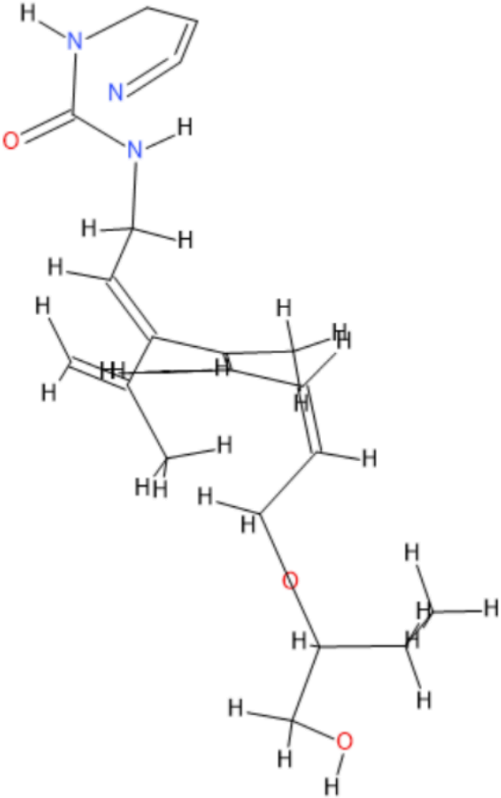
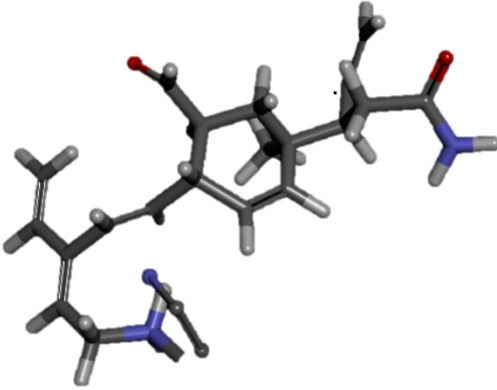
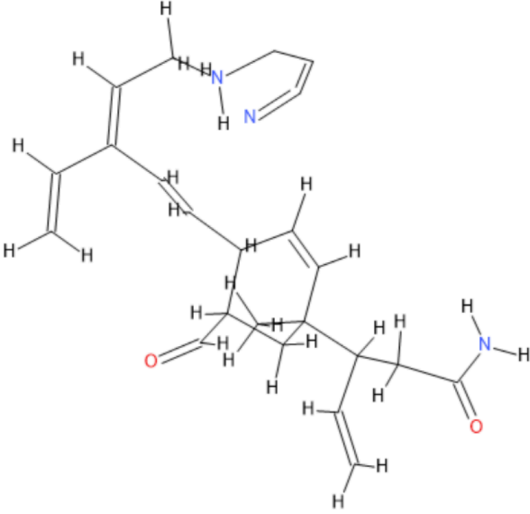
Structure	Family 12	Properties
3D		<p>Molecular weight: 338</p> <p>LogP: 4.88</p> <p>pKd: 8.47</p> <p>HBA: 4</p> <p>HBD: 2</p>
2D		

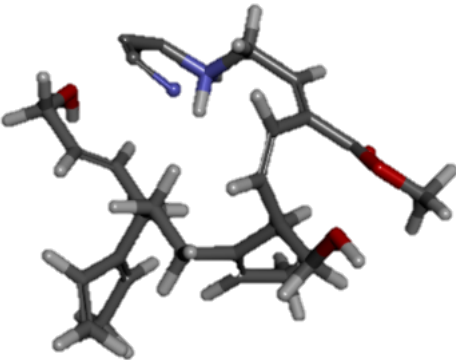
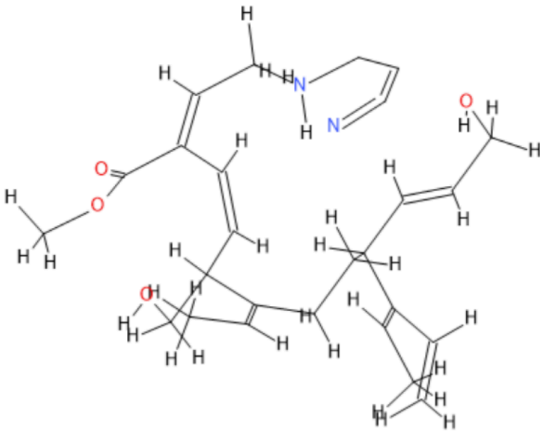
Table 3.5: 2D and 3D structures of the **highest** affinity generated molecules from **Seed 2**; together with its corresponding properties. Images rendered in Discovery Studio^{®5} and BIOVIA Accelrys

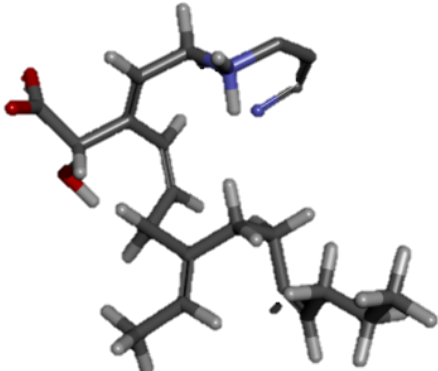
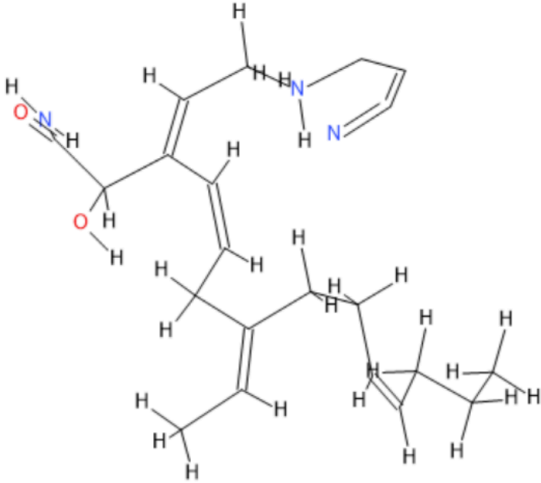
Draw^{®6}

Structure	Family 1	Properties
3D		<p>Molecular weight: 410</p> <p>LogP: 4.46</p> <p>pKd: 9.7</p> <p>HBA: 5</p> <p>HBD: 5</p>
2D		

Structure	Family 2	Properties
3D		<p data-bbox="1098 804 1394 840">Molecular weight: 395</p> <p data-bbox="1098 887 1235 922">LogP: 4.54</p> <p data-bbox="1098 965 1222 1001">pKd: 9.33</p> <p data-bbox="1098 1043 1187 1079">HBA: 4</p> <p data-bbox="1098 1122 1187 1158">HBD: 4</p>
2D		

Structure	Family 3	Properties
3D		<p>Molecular weight: 378</p> <p>LogP: 4.65</p> <p>pKd: 9.28</p> <p>HBA: 3</p> <p>HBD: 3</p>
2D		

Structure	Family 5	Properties
3D		<p>Molecular weight: 439</p> <p>LogP: 4.94</p> <p>pKd: 9.17</p> <p>HBA: 5</p> <p>HBD: 4</p>
2D		

Structure	Family 6	Properties
3D		<p>Molecular weight: 356</p> <p>LogP: 4.32</p> <p>pKd: 9.18</p> <p>HBA: 4</p> <p>HBD: 4</p>
2D		

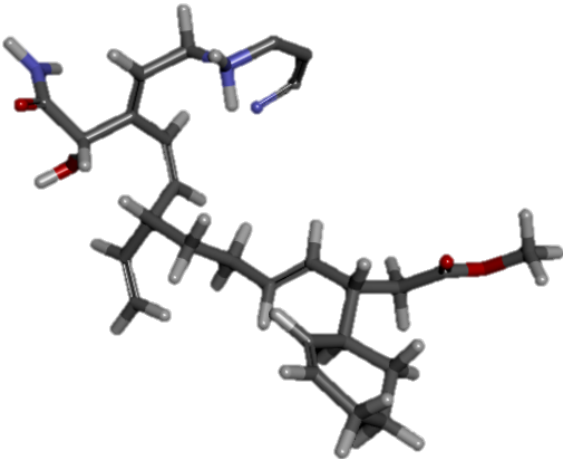
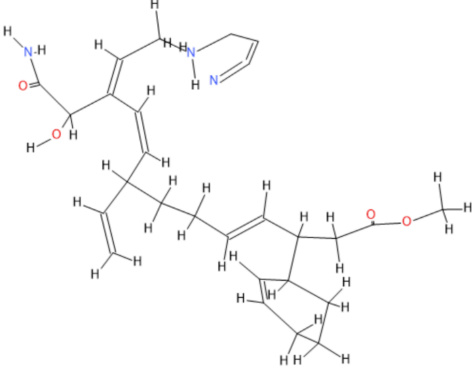
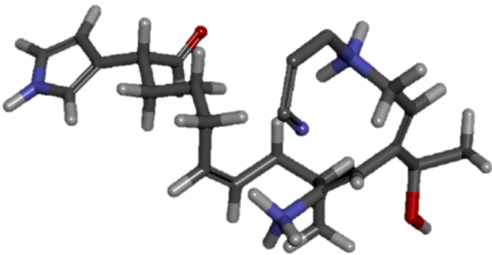
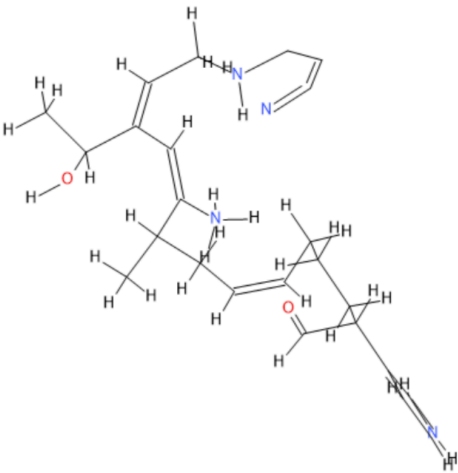
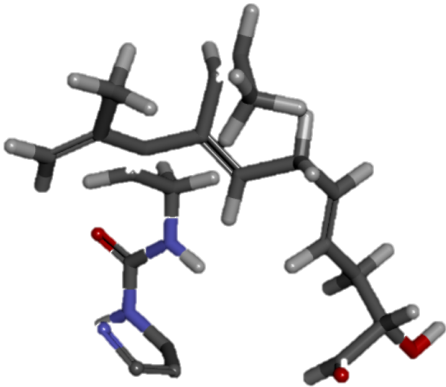
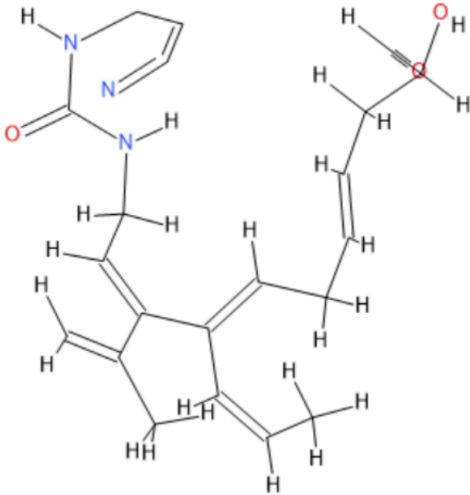
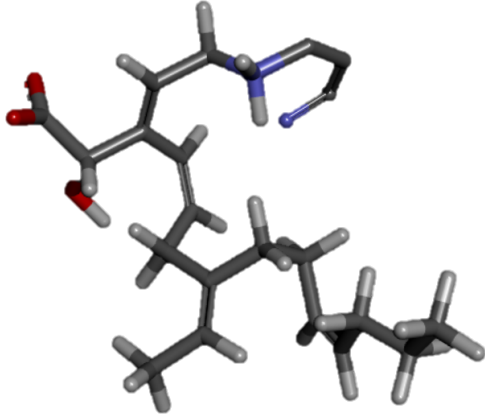
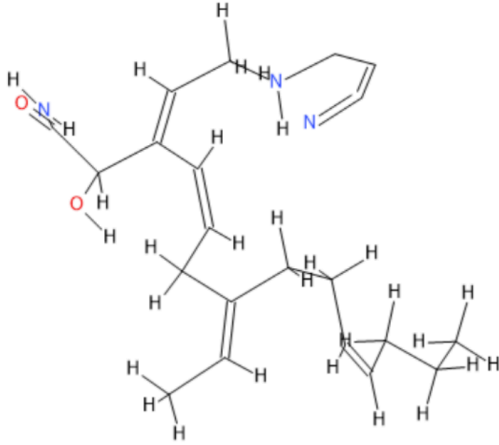
Structure	Family 8	Properties
3D		<p>Molecular weight: 466</p> <p>LogP: 4.92</p> <p>pKd: 9.51</p> <p>HBA: 5</p> <p>HBD: 4</p>
2D		

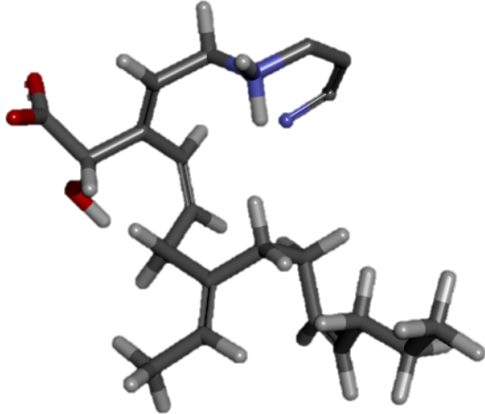
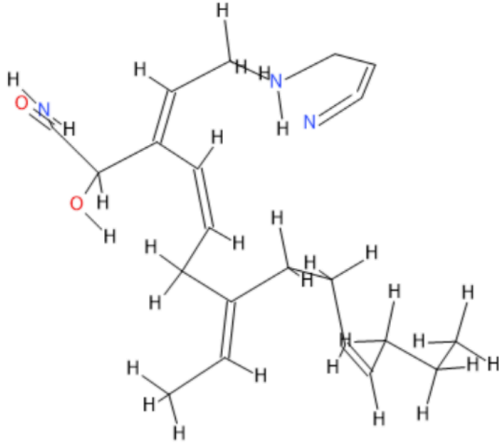
Table 3.6: 2D and 3D structures of the **lowest** affinity generated molecules from **Seed 2**; together with its corresponding properties. Images rendered in Discovery Studio^{®5} and BIOVIA Accelrys

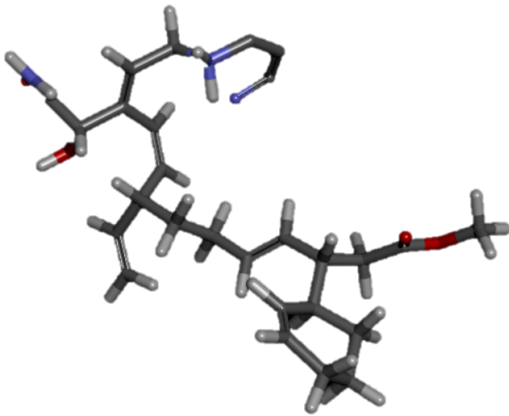
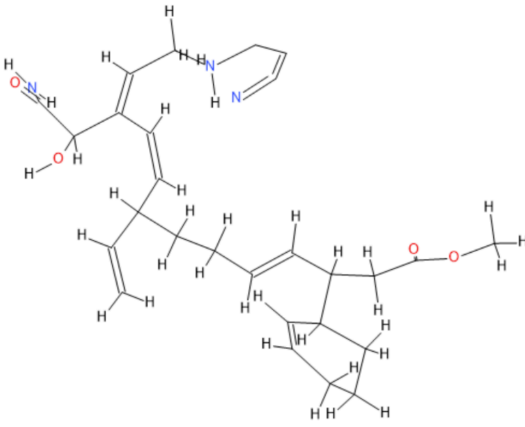
Draw^{®6}

Structure	Family 1	Properties
3D		<p>Molecular weight: 410</p> <p>LogP: 4.87</p> <p>pKd: 9.11</p> <p>HBA: 5</p> <p>HBD: 5</p>
2D		

Structure	Family 2	Properties
3D		<p>Molecular weight: 367</p> <p>LogP: 4.97</p> <p>pKd: 9.23</p> <p>HBA: 4</p> <p>HBD: 4</p>
2D		

Structure	Family 6	Properties
3D		<p>Molecular weight: 356</p> <p>LogP: 4.64</p> <p>pKd: 9.18</p> <p>HBA: 4</p> <p>HBD: 4</p>
2D		

Structure	Family 6	Properties
3D		<p>Molecular weight: 356</p> <p>LogP: 4.64</p> <p>pKd: 9.18</p> <p>HBA: 4</p> <p>HBD: 4</p>
2D		

Structure	Family 8	Properties
3D		<p>Molecular weight: 466</p> <p>LogP: 4.92</p> <p>pKd: 9.37</p> <p>HBA: 5</p> <p>HBD: 4</p>
2D		

Chapter 4

Discussion

4.0 Discussion

Literature suggests that the Glutaminase C receptor is a potential target for impeding cancer cell growth and proliferation. This study produced two molecular cohorts of high affinity for Glutaminase C through two distinct approaches; ligand-based and structure-based drug design. Structure-based drug design uses known information regarding the 3D structure of the target, which is obtained from the Protein Data Bank (containing information concerning several molecules acquired by X-Ray crystallography and NMR spectrometry) in order to design novel molecules. Both methods which were utilised in this project, *de novo* and Virtual Screening (VS), have their own several features.

The affinity of the two cohorts cannot be compared due to the different underlying assumptions and parameters inherent to each approach. Reference is made to table 4.1, where the differences between *de novo* design and VS are highlighted.

Table 4.1: Table comparing *de novo* and VS approach

<i>de novo</i>	VS
Less innovative	Highly innovative
More limitations; due to smaller ligand binding pocket utilised	Broader-based (no structural limitations)
More restricted ligand population can be acquired – however greater chance of success	More varied ligand population can be acquired – however lower chance of success

Specifically, in this study the results obtained through VS are more structurally diverse than those obtained through *de novo* design. This is due to the fact that in VS, a general pharmacophore was used, which afforded the recruited hit structures significant diversity as long as they complied with the modelled consensus pharmacophore.

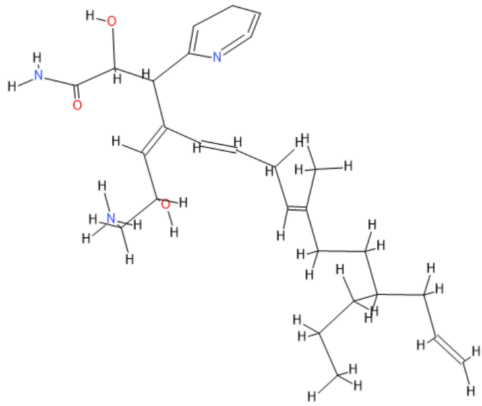
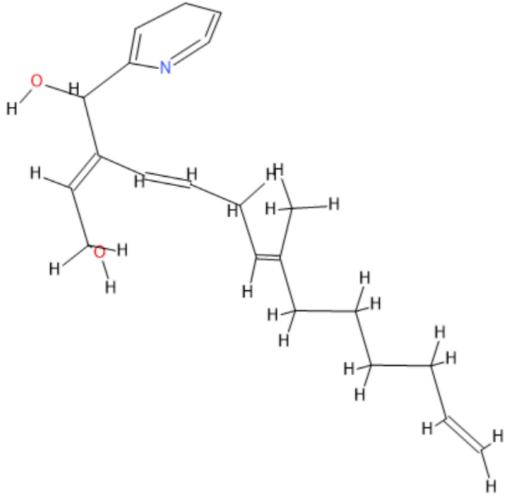
In *de novo* design, there is a much greater homogeneity of results. This may be attributed to the fact that the design process is emanated from pre-modelled seed structures that always formed part of the *de novo* structures.

The structural restrictions of the *de novo* designed molecules is offset by the fact that those were modelled in an area of the Glutaminase C receptor that is known to be bioactive. The *de novo* designed molecules consequently have a higher propensity to bioactivity than their VS identified counterparts which were docked into a virtual LBP that was much larger than the zone known to be bioactive and described in PDB crystallographic deposition 5HL1 (Huang & Cerione, 2016).

The two molecular cohorts obtained, while being incomparable from an affinity perspective, should be seen as being complementary to each other with one cohort compensating for the limitations of the other. This is an advantage from a drug design perspective, because it provides for a strong point of departure from which further rounds of optimisation can identify the strongest druggable candidate. This study was limited by the fact that that it was carried out in a static environment. In fact, in planning for future research, molecular dynamic simulations which compare the motions of the identified and designed structures within the Glutaminase C LBP with those of known inhibitors should be carried out.

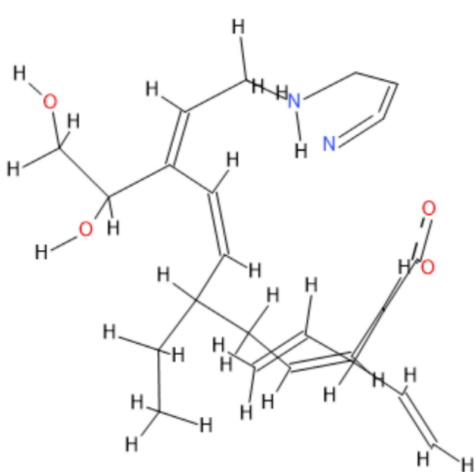
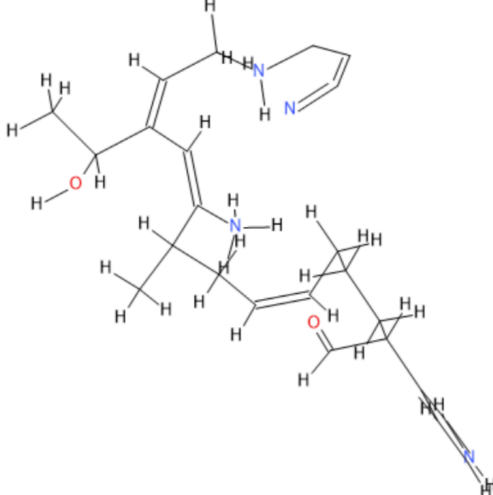
Two seed structures were obtained through the *de novo* approach. For **Seed 1**, a total of 10 Lipinski Rule compliant families were created, with Molecule 2 from Family 1 having the highest affinity and Molecule 73 from Family 6 with the lowest affinity to the ligand binding pocket.

Table 4.2: Table comparing molecules obtained from Seed 1 with the highest and lowest affinity to the ligand binding pocket

	Highest Affinity	Lowest Affinity
Seed 1		
	<ul style="list-style-type: none"> • Molecule 2 • Family 1 • Affinity: 9.98 	<ul style="list-style-type: none"> • Molecule 73 • Family 6 • Affinity: 4.89

For **Seed 2**, a total of 6 Lipinski Rule compliant families were created, with Molecule 23 from Family 1 having the highest affinity and Molecule 95 from Family 1 with the lowest affinity.

Table 4.3: Table comparing molecules obtained from Seed 2 with the highest and lowest affinity to the ligand binding pocket

	Highest Affinity	Lowest Affinity
Seed 2		
	<ul style="list-style-type: none"> • Molecule 23 • Family 1 • Affinity: 9.7 	<ul style="list-style-type: none"> • Molecule 95 • Family 1 • Affinity: 4.87

Through the *de novo* approach, Seed 1 showed superiority over Seed 2. The ligands obtained from Seed 1 showed a greater affinity (pKd: 9.98) towards the Ligand Binding Pocket compared to Seed 2 (pKd: 9.7), as seen in Tables 4.4 and 4.5 respectively.

Table 4.4: Highest affinity generated molecules from Seed 1 through the de novo approach

ID	Family	Molecular Weight	Calculated LogP	Binding Score (pKd)	Chemical Score	HBA	HBD
2	1	452	4.48	9.98	-100	4	4
5	1	394	4.42	9.83	-90	5	3
6	1	392	4.97	9.83	-120	5	3

Table 4.5: Highest affinity generated molecules from Seed 2 through the de novo approach

ID	Family	Molecular Weight	Calculated LogP	Binding Score (pKd)	Chemical Score	HBA	HBD
23	1	410	4.46	9.7	-100	5	5
26	1	385	4.87	9.66	-90	3	5
28	1	412	4.6	9.65	-90	3	5

In order to gain knowledge regarding the amino acids which are critical to binding and in the design of Glutaminase C modulators, the interactions with PDB crystallographic depositions 5HL1 (Huang & Cerione 2016), 5WJ6 (Huang *et al.*, 2018) and the highest affinity molecule obtained through *de novo* design, C₂₇H₃₈N₃O₃ (Seed 1, Molecule 2, Family 1; pKd 9.98) were analysed through the creation of 2D topology maps.

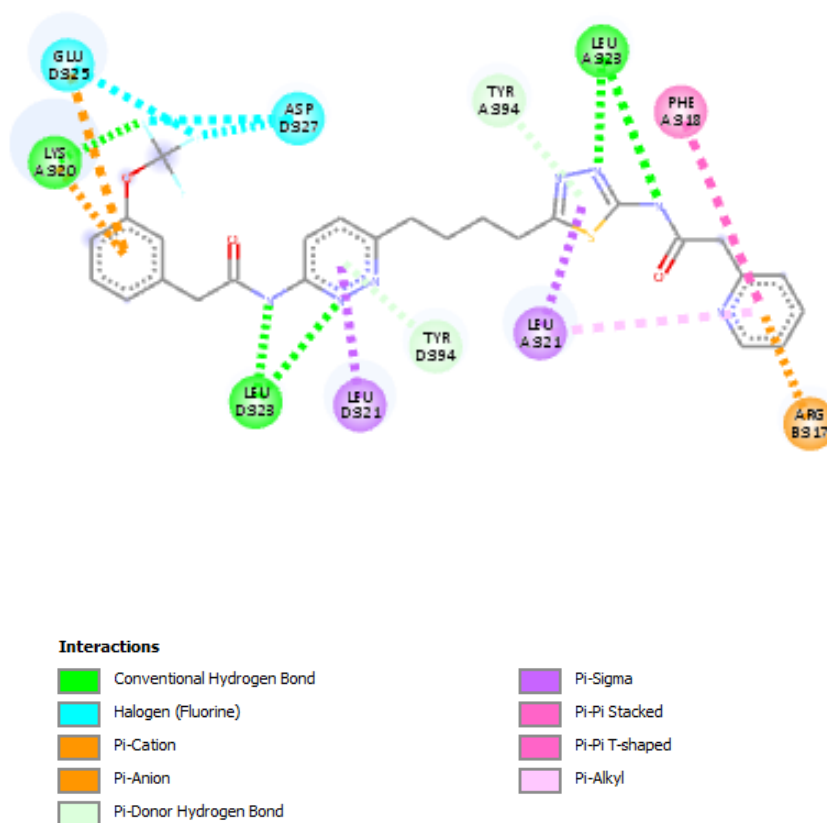


Figure 4.1: Topology map of PDB crystallographic deposition 5HL1
generated in Discovery Studio®

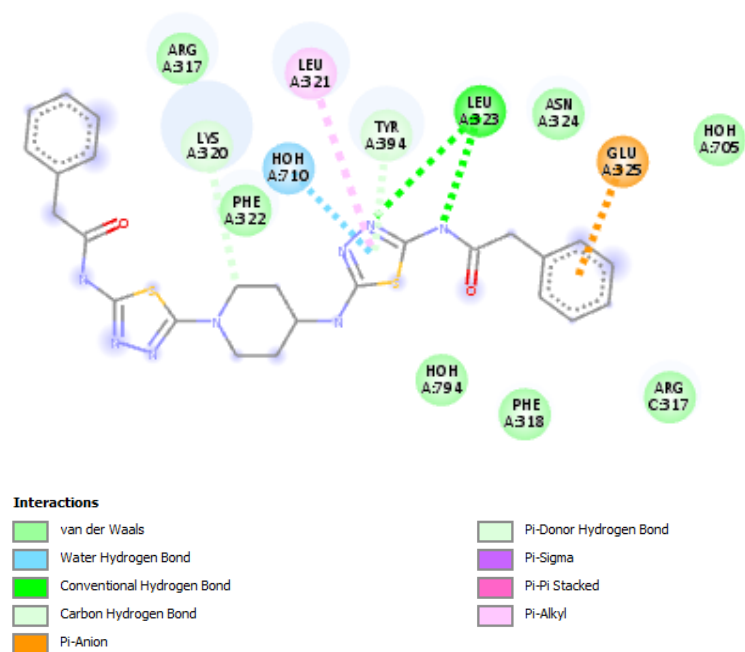


Figure 4.2: Topology map of PDB crystallographic deposition 5WJ6 generated in Discovery Studio®

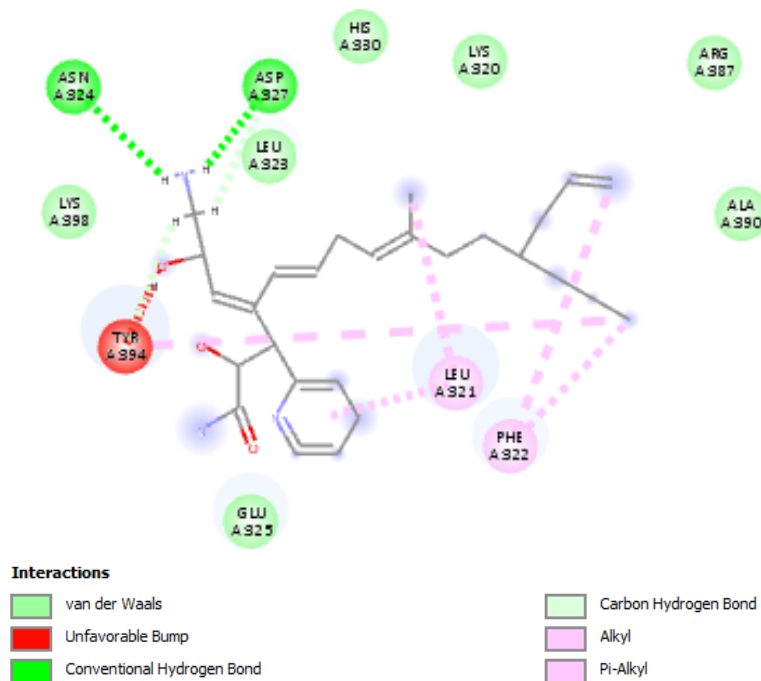


Figure 4.3: Topology map of the best de novo molecule, $C_{27}H_{38}N_3O_3$ generated in Discovery Studio®

The interactions of the highest affinity *de novo* molecule (C₂₇H₃₈N₃O₃) with the receptor is probably due to the following amino acid interactions: HIS³³⁰, ASP³²⁷, LYS³⁹⁸, ALA³⁹⁰, ARG³⁹⁷, ASP³²⁷ AND PHR³²².

This probably accounts for the superior affinity that this has for the Glutaminase C LBP.

In the design of higher affinity molecules, the interactions obtained with the highest affinity *de novo* molecule, C₂₇H₃₈N₃O₃, should be maintained. Therefore, these amino acids are of utmost importance to the target when verifying the biological activity through *in vitro* assays.

The superior ligands obtained from VS together with the optimal molecules obtained from the *de novo* approach will be further optimised to analyse whether they are efficacious enough to become potential ligands for clinical use.

References

Benet LZ, Hosey CM, Ursu O, Oprea TI. BDDCS, the Rule of 5 and drugability. *Advanced Drug Delivery Reviews*. 2016;101:89-98.

Berman H, Bhat T, Bourne, P, Feng Z, Gilliland G, Weissig H, et al. Journal search results - *Nature Structural Biology*. 2000;7:957-959.

Boysen G, Jamshidi-Parsian A, Davis M, Siegel E, Simecka C, Kore R et al. Glutaminase inhibitor CB-839 increases radiation sensitivity of lung tumor cells and human lung tumor xenografts in mice. *International Journal of Radiation Biology*. 2018;:1-7.

Cassago A, Ferreira A, Ferreira I, Fornezari C, Gomes E, Greene K et al. Mitochondrial localization and structure-based phosphate activation mechanism of Glutaminase C with implications for cancer metabolism. *Proceedings of the National Academy of Sciences*. 2012;109(4):1092-1097.

Certara USA, Inc. SYBYL-X. Version 2.1. 103 Carnegie Center, Suite 300, Princeton, NJ 08540 USA.

Ferlay J, Shin H, Bray F, Forman D, Mathers C, Parkin D. Estimates of worldwide burden of cancer in 2008: GLOBOCAN 2008. *International Journal of Cancer*. 2010;127(12):2893-2917.

Gross M, Demo S, Dennison J, Chen L, Chernov-Rogan T, Goyal B et al. Antitumor Activity of the Glutaminase Inhibitor CB-839 in Triple-Negative Breast Cancer. *Molecular Cancer Therapeutics*. 2014;13(4):890-901.

Guo Y, Yu S, Zhang C, Kong A. Epigenetic regulation of Keap1-Nrf2 signaling. *Free Radical Biology and Medicine*. 2015;88:337-349.

Guo L, Zhou B, Liu Z, Xu Y, Lu H, Xia M et al. Blockage of glutaminolysis enhances the sensitivity of ovarian cancer cells to PI3K/mTOR inhibition involvement of STAT3 signaling. *Tumor Biology*. 2016;37(8):11007-11015.

Huang Q, Cerione R. Crystal structure of glutaminase C in complex with inhibitor CB-839. 2016.

Huang Q, Stalneck C, Zhang C, McDermott L, Iyer P, O'Neill J et al. Characterization of the interactions of potent allosteric inhibitors with glutaminase C, a key enzyme in cancer cell glutamine metabolism. *Journal of Biological Chemistry*. 2018;293(10):3535-3545.

Hilbig M., Rarey M. MONA 2: a light cheminformatics platform for interactive compound library processing. *J. Chem. Inf. Model.* 2015; 55(10): 2071–2078.

Jacque N, Ronchetti A, Larrue C, Meunier G, Birsén R, Willems L et al. Targeting glutaminolysis has antileukemic activity in acute myeloid leukemia and synergizes with BCL-2 inhibition. *Blood.* 2015;126(11):1346-1356.

Jorgensen WL. The many roles of computation in drug discovery. *Science* 2004 Mar 19;303(5665):1813-1818. Accessed January 10th, 2020.

Katt W, Ramachandran S, Erickson J, Cerione R. Dibenzophenanthridines as Inhibitors of Glutaminase C and Cancer Cell Proliferation. 2018.

Koes D.R & Camacho J.C. ZINCPharmer: pharmacophore search of the ZINC database. *Nucleic Acids Res* (2012), 2012 May; 40(W1): W409-W414.

Lipinski CA, Lombardo F, Dominy BW, Feeney Pj. Experimental and computational approaches to estimate solubility and permeability in drug discovery and development settings. *Advanced Drug Delivery Reviews* 2015; 46(1-3):3-26.

Lung Cancer (Non-Small Cell) [Internet]. 2018 [cited 15 February 2020]. Available from:<http://www.dotscanada.com/wp-content/uploads/2011/12/About-Cancer.pdf>

Matre P, Velez J, Jacamo R, Qi Y, Su X, Cai T et al. Inhibiting glutaminase in acute myeloid leukemia: metabolic dependency of selected AML subtypes. *Oncotarget*. 2016;7(48).

Momcilovic M, Bailey S, Lee J, Fishbein M, Magyar C, Braas D et al. Targeted Inhibition of EGFR and Glutaminase Induces Metabolic Crisis in EGFR Mutant Lung Cancer. *Cell Reports*. 2017;18(3):601-610.

Okamoto T, Suzuki Y, Fujishita T, Kitahara H, Shimamatsu S, Kohno M et al. The prognostic impact of the amount of tobacco smoking in non-small cell lung cancer—Differences between adenocarcinoma and squamous cell carcinoma. *Lung Cancer*. 2014;85(2):125-130.

Parlati F, Demo S, Gross M, Janes J, Lewis E, MacKinnon A et al. Abstract 1416: CB-839, a novel potent and selective glutaminase inhibitor, has broad antiproliferative activity in cell lines derived from both solid tumors and hematological malignancies. *Cancer Research*. 2014;74(19 Supplement):1416-1416.

Proekt A, Hemmings H. Mechanisms of Drug Action. *Pharmacology and Physiology for Anesthesia*. 2013;:3-19.

Ramucirumab - DrugBank [Internet]. Drugbank.ca. 2018 [cited 25 February 2020]. Available from: <https://www.drugbank.ca/drugs/DB05578>

Romero R, Sayin V, Davidson S, Bauer M, Singh S, LeBoeuf S et al. Keap1 loss promotes Kras-driven lung cancer and results in dependence on glutaminolysis. *Nature Medicine*. 2017;.

Sasaki H, Suzuki A, Shitara M, Okuda K, Hikosaka Y, Moriyama S et al. Keap1 mutations in lung cancer patients. *Oncology Letters*. 2013;6(3):719-721.

Siegel, R., Miller, K. and Jemal, A., 2020. Cancer statistics, 2020. *CA: A Cancer Journal for Clinicians*, 70(1), pp.7-30.

Stierand K, Rarey M. PoseView -- molecular interaction patterns at a glance. *Journal of Cheminformatics*. 2010;2(Suppl 1):P50.

Thangavelu K, Chong Q, Low B, Sivaraman J. Structural Basis for the Active Site Inhibition Mechanism of Human Kidney-Type Glutaminase (KGA). *Scientific Reports*. 2014;4(1).

Tiwari MK, Singh R, Singh RK, Kim IW, Lee JK. Computational approaches for rational design of proteins with novel functionalities. *Comput Struct Biotechnol J* 2012 Sep 28; 2:e201209002. Accessed February 2nd, 2020.

Trametinib | STEMCELL Technologies [Internet]. Stemcell.com. 2018 [cited 10th February 2020]. Available from: <https://www.stemcell.com/trametinib.html>

Vogl D, Younes A, Stewart K, Orford K, Bennett M, Siegel D et al. Phase 1 Study of CB-839, a First-in-Class, Glutaminase Inhibitor in Patients with Multiple Myeloma and Lymphoma [Internet]. Blood Journal. 2019 [cited 13 February 2020]. Available from: http://www.bloodjournal.org/content/126/23/3059?sso-checked=true&utm_source=TrendMD&utm_medium=cpc&utm_campaign=Blood_TrendMD_0

Wolber G, Langer T. LigandScout: 3-D Pharmacophores Derived from Protein-Bound Ligands and Their Use as Virtual Screening Filters. Journal of Computer-Aided Molecular Design. 2005; 45(1); 160-169.

Wong M, Lao X, Ho K, Goggins W, Tse S. Incidence and mortality of lung cancer: global trends and association with socioeconomic status. Scientific Reports. 2017;7(1).

Xiang Y, Stine Z, Xia J, Lu Y, O'Connor R, Altman B et al. Targeted inhibition of tumor-specific glutaminase diminishes cell-autonomous tumorigenesis. Journal of Clinical Investigation. 2015;125(6):2293-2306.

Yuan Y, Pei J, Lai L. LigBuilder 2: A Practical de Novo Drug Design Approach. Journal of Chemical Information and Modeling. 2011;51(5):1083-109.

List of Publications and Abstracts

Abstract submitted to the:

- 20th Medicinal and Pharmaceutical Sciences Congress, August 30-31st 2021, Japan
- Drug Design and Development, October 14-15th 2021, Webinar
- Pharmaceutical Chemistry and Drug Design, September 21st 2021, Webinar
- Journal of Biochemistry

Title *	Ms
First Name *	Lara
Last Name	Zammit
Country *	Malta
Author's Email *	lara.z.zammit.16@um.edu.mt
Phone Number *	99527292
Abstract Category *	Poster
Track Name *	Drug Development

Title: Rational Design and Preliminary Validation of Glutaminase C Modulators

Name: Lara Zammit

University of Malta, Faculty of Medicine and Surgery, Department of Pharmacy

Glutaminolysis is a process which drives cell proliferation in tumours. This process is driven by Glutaminase C (Gc). Literature indicates that Gc is over-expressed in solid tumours mainly those of the lung and that its antagonism could inhibit tumour growth. The objective in this study is to design & identify novel Gc modulators through Virtual Screening (VS) & de novo design.

The design of this project uses high affinity Gc inhibitor experimental molecule CB-839, was used as a lead for the identification of optimised analogues using VS. A consensus pharmacophore was generated by superimposing pharmacophores of inhibitor molecules obtained from PBD crystallographic depositions 5HL1 & 5WJ6 using Ligand Scout®. Sybyl-X® was used to model a protomol; followed by docking of hits obtained through VS. The ligand binding affinities of the 2 hit molecular structures were calculated in Sybyl-X®. de novo approach was used to design novel modulators, where seed structures derived from CB-839 were modelled and allowed growth within the CB-839 ligand binding pocket (LBP). The main outcome of this project is to obtain two molecular cohorts of high affinity lead like Gc modulators.

Through virtual screening, 2 high affinity lead-like molecules were yielded; which are structurally diverse from the lead. CB-839 derived seeds were modelled and will be docked into Gc LBP in de novo phase.

This study was valuable in modelling a unique pharmacophore that explored maximal pharmacophoric space using VS. The de novo design was used as a complementary approach. The optimal structures will be optimised further.

Biography

Lara Zammit attends University of Malta and is currently reading for a Master's degree in Pharmacy. She just finished her Bachelor of Science degree in Pharmaceutical Science in 2020. Currently, working at a pharmacy to gain experience prior to getting her warrant which allows pharmacy students to practice in any European country.

Presenting author details

Full name: Lara Zammit

Contact number:00356 99527292

Linked In account: <https://www.linkedin.com/in/lara-zammit-81833b193/>

Category: (Oral presentation/ Poster presentation) Poster Presentation

Draft Manuscript For Review

Rational Design and Preliminary Validation of Glutaminase C Modulators

Journal:	<i>The Journal of Biochemistry</i>
Manuscript ID	Draft
Manuscript Type:	Rapid Communication
Date Submitted by the Author:	n/a
Complete List of Authors:	Zammit, Lara; University of Malta, Faculty of Medicine and Surgery, Department of Pharmacy
Keywords:	Drugs < Pharmacology, Metabolism, Lung < Tissue/organ Systems, Cancer < Diseases, Pharmacology
Topics:	01 Biochemistry General < BIOCHEMISTRY

SCHOLARONE™
Manuscripts